

Supplementary Material- Paleoenvironmental and biotic changes in the Late Triassic of Argentina: testing hypotheses of abiotic forcing at the basin scale

Paleoenvironment

Table S1. Facies associations and their characteristics are defined for the Ischigualasto Formation (Late Triassic) at the Cerro Bola locality, the Ischigualasto-Villa Unión Basin, Argentina. The sedimentological analysis consisted of determining facies defined by sedimentary structures and textures and recorded using the acronyms of the lithofacies code proposed by Miall (1996). Facies associations were identified to interpret the environments and sub-environments. The Rock Color Chart of the Geological Society of America (GSA 1948) was used for color descriptions.

Facies Association Interpretation	Litho-facies	Lithology	Color (Rock-color Chart)	Sedimentary structure	Bed geometry	Thickness (T) and lateral extension (W)	Fossil content	Other features	Processes and interpretation	Lateral and vertical relations
Channel multistory	Gm	Conglomerate Clast-support, moderate-sorted, clast from 0.5 cm- 10cm (Q, Feld, Lithic, Volcanic, Rhyolite)	5Y2/1, 5Y7/2, 5Y6/4, 5Y3/2, 5Y5/2, 10Y6/2	Structureless-lag	Lenticular-lentiform erosional basal boundaries	T: 1.7-19.3 m W: several to tens meters Individual bed T:0.5-2 m	Invertebrate trace, wood	Micro-concretions on top of different sized (2-8 cm)	Tractive flow Lag and channel bar	Overlie Floodplain and Levee FA and overlain by Floodplain, Levee and Crevasse splay FA
	Gh	Horizontal stratification		Tractive flow Channel bar						
	Gp	Planar-cross-stratification		Tractive flow Channel bar						
	Sp	Planar-cross-stratification		2-D dune migration						
	St	Trough-cross-stratification		3-D dune migration						
	Glag	Conglomerate Clast-support, moderate-sorted, clast from 0.5 cm- 10cm (Q, Feld, Litic, Volcanic, Riolite)		Structureless-lag					Tractive flow Lag	
Channel Single-story	Sp	Medium- to coarse-grained sandstone (Q, Feld)	N8, 5Y8/4, 5Y7/2, 5Y5/6, 5GY5/2, 10Y6/2, 10YR6/2	Lenticular-lentiform erosional basal boundaries	T: 1-7.45 m W: several to tens meters Individual bed T:		Nodule-concretions on top of different sized (2-8 cm)		Tractive flow Lag	Overlie Floodplain and Levee FA and overlain by Floodplain and Levee FA
	St									
Levee	Sm	Fine- to medium-grained sandstone	N8, 5Y6/1, 5Y7/2, 5Y5/2, 5Y5/6, 5Y4/4, 5YR4/1, 5GY5/2,	Structureless	Tabular	T: 1-5.6 m W: tens to hundred meters Individual bed T:0.1-0.2 m		Banded	Tractive flow	Overlie Channel multistory and single-story FA and overlain by Channel

	Sh		5GY7/2, 5R2/2, 5R4/2, 10Y6/2, 10Y5/4, 10YR6/2, 10GY5/2	Horizontal lamination				Tractive flow Planar bed flow	multistory and single-story, Crevasse channel, Crevasse splay, and Floodplain FA	
Crevasse Channel	Sp	Fine- to medium- grained sandstone	5Y5/2, 5Y6/4, 10Y4/2, 10YR6/2	Planar-cross- stratification	Lenticular- tabular	T: 0.4-1.6 m W: several to tens meters		2-D dune migration	Overlie Floodplain and Levee FA and overlain by Floodplain FA	
	Sm			Structureless				Tractive flow		
	Sr			Ripple lamination				Tractive flow Ripple flow		
Crevasse splay	Sh	Fine- to medium- grained sandstone	N8, 5y3/2, 5Y6/4, 5Y6/1, 5Y5/2, 5Y7/2, 5GY5/2, 5GY4/1, 5YR6/1, 5R6/2, 5R2/2, 10Y6/2, 10GY5/2, 10YR2/2, 10R4/2	Horizontal lamination	Lentiform- tabular	T: 0.1-1.5 m W: tens to hundred meters		Tractive flow Planar bed flow	Overlie Floodplain and Levee FA and overlain by Floodplain FA	
	Sm			Structureless				Tractive flow		
	Sr			Ripple lamination				Tractive flow Ripple flow		
Floodplain	Fl-Fm	Very fine-grained sandstone to mudstone	N3, 5Y5/2, 5Y3/2, 5Y2/1, 5Y4/1, 5YR2/1, 5YR3/2, 5YR5/2, 5YR3/4, 5GY5/2, 5GY3/2, 5GY6/1, 5GY7/2, 5G5/2, 5R2/2, 5R4/2, 5P4/2, 10Y6/2, 10Y4/2	Horizontal lamination- Structureless	Tabular	T: 0.6-21 m W: hundred meters	Vertebrates, plants, root cast,	Mottle, banded, ped, concretions, slickensides, black lens	Suspension	Overlie Crevasse channel, Crevasse splay, Levee, Channel Multistory and Single-story FA and overlain by Crevasse channel, Crevasse splay, Levee, Channel Multistory, and Single-story FA

Clay mineralogy

X-Ray Diffraction: The mineralogical composition of samples was analyzed with x-ray diffraction (XRD) of the <2 µm sample fraction using a PANalytical X’Pert PRO diffractometer of the Research Center (La Plata, Argentina). The rocks samples were disaggregated and powdered in an agate mortar. Clay minerals (Table S2) were obtained by pipetting the fraction <2 µ in a suspension with distilled water following the Stokes Law. The samples were prepared according to the glass slide method: a) natural, air-dried sample in the laboratory at environment temperature; b) glycolated, sample exposed to the vapors of an ethylene glycol solution for at least 24 h; c) calcined, the sample taken at 550°C for two hours. X-ray diffraction patterns were obtained using Cu K-alpha radiation ($k\alpha=1.5403 \text{ \AA}$) operated at 40 kV, 40 mA, and scanning speed of 0.04°/s, between 4° to 37° 2θ, for the total rock samples; among 2° to 32° for the natural samples of the clay fraction; 2° to 27° for the glycolated samples of that same fraction, and 3° to 15° for the calcined samples were scanned. For mixed-layer illite/smectite, the contribution of illite was determined by the Reichweite value (R) calculated following Moore and Reynolds (1997).

Ischigualasto clay mineralogy

Illite is recorded throughout the section; it is absent in only a few samples. It dominates the assemblages and is the only clay recorded from ~100 to 200 m (Figure 2, Table S2). Smectite is recorded in the first ~ 50 m section as smectite or mixed-layer illite/smectite with Reichweite values of R1 and R2. Up-section, from ~50 to 200 m, smectite is absent but is recorded again from ~200 to 800 m, where it is predominantly smectite and to a lesser extent as mixed-layer illite/smectite with a value of R3 (Figure 2, Table S2). This mixed-layer illite/smectite has a variable occurrence throughout the section (Figure 2, Table S2). Kaolinite shows a similar distribution to smectite, being absent between ~110 to ~380 m.

The assemblages recorded in the Ischigualasto Formation at Cerro Bola North can be described in four main assemblage groups. On the one hand, the clay assemblages from samples IB 20-28, 33, and 38 composed exclusively of illite are found in floodplain deposits with paleosol development. The second group (samples IB7, 16, 30, 34-36, 39, 51, 58, 68, 70-81, 85-87, 127) includes different proportions of illite, mixed-layer illite/smectite, smectite, and trace amounts chlorite (Figure 2, Table S2); these are also from floodplain deposits with paleosol development. In general, the dominant component is illite, followed by smectite and mixed-layer illite/smectite, whereas chlorite is found only in a few samples (Figure 2, Table S2). Mixed-layer illite/smectite mostly has a value of R3 with approximately 75% illite; therefore, the smectite composition is 25%. The third assemblage, recorded in both lacustrine and floodplain deposits, is dominated by illite with some kaolinite (samples IB18, 19, 89, and at the top of the Los Rastros Formation: IB2). Finally, the fourth assemblage, from floodplain deposits with paleosol development, included different proportions of illite, mixed-layer illite/smectite, smectite, and kaolinite. The mixed-layer illite/smectite in these samples (R3 value) is predominantly composed of illite.

Table S2. XRD-based Phyllosilicate composition expressed in % of the clay fraction from the mudstone facies of the Ischigualasto Formation at the Cerro Bola locality, Ischigualasto-Villa Union Basin, Argentina.

Sample	Section (m)	Clay mineralogy (%)				
		Kaolinite	Illite	Illite/Smectite	Smectite	Chlorite
IB2	2.00	30	70			
IB3	3.00	26	55		19	
IB5	11.50	15	47	38		
IB7	21.50			100		
IB10	34.00	19	51	30		
IB11	36.50	13	57		17	13
IB14	38.50	16	56	28		
IB16	43.00		60	40		
IB17	43.50	24	60		16	
IB18	72.50	19	81			
IB19	73.00	30	70			
IB20	112.00		100			
IB25	174.50		100			
IB26	177.00		100			
IB27	213.00		100			
IB28	213.50		100			
IB30	231.00		58	42		
IB33	253.00		100			
IB34	254.00		71		29	
IB35	309.50		55	29		16
IB36	318.00		67	33		
IB38	363.00		100			
IB39	370.00		81		19	
IB41	395.00	43			57	
IB44	420.00	35			65	
IB47	430.00	18	46		36	
IB51	441.00		58	42		
IB55	465.00	40			60	
IB58	466.50		62	38		
IB60	477.00	16	54	30		
IB63	485.00		74		26	
IB67	490.00	16	39		45	
IB70	498.00		62	38		
IB74	509.00		63	37		
IB77	520.00		62	38		
IB81	537.50		74	26		
IB84	548.00	30			70	
IB85	553.50		65	35		
IB87	557.00		100			
IB89	562.50	28	72			
IB93	582.50	40			60	
IB96	588.50	25	53		22	
IB99	593.00	21	56	23		
IB102	611.50	25	57		18	
IB106	619.50	21	53		26	
IB107	632.00	33	36		31	
IB109	645.50	23	51		26	

IB114	661.50	18	45		37	
IB118	682.00	38			62	
IB120	687.00	23	51		26	
IB126	744.50	14	42	28	16	
IB127	759.00		72		28	

Mineralogical proxies

Ischigualasto mineralogical proxies

The kaolinite/illite ratio displays values between 0 and 0.923, with higher values and high dispersion in the first ~100 m and upper ~380 m of the section (Figure 2; Table S3). The smectite/illite ratio displays values between 0 to 1.163 (Figure 2; Table S3), with low values and moderate dispersion in the first ~100 m, and low values and low dispersion between ~100 to 380 m, but high values with high dispersion upper ~380 m of the section. The smectite/kaolinite ratio display values between 0 to 2.812 (Figure 2; Table S3), with low values and dispersion in the first ~100 m and variable values with high dispersion above ~380 m in the section.

Table S3. Mineralogical proxies were calculated based on clay fractions from the mudstone facies of the Ischigualasto Formation at the Cerro Bola locality, Ischigualasto-Villa Union Basin, Argentina.

Kaolinite/illite ratio reflects the intensity of chemical weathering, smectite/illite ratio reflects the increase of chemical weathering under seasonal climates, and smectite/kaolinite ratio reveals a history of chemical versus physical weathering rates.

Sample	Section (m)	Kaolinite/illite	Smectite/illite	Smectite/Kaolinite
IB2	2.00	0.430232558	0	0
IB3	3.00	0.464566929	0.338582677	0.728813559
IB5	11.50	0.312977099	0	0
IB7	21.50			
IB10	34.00	0.363636364	0	0
IB11	36.50	0.227272727	0.303030303	1.333333333
IB14	38.50	0.287323944	0	0
IB16	43.00	0	0	0
IB17	43.50	0.390625	0.265625	0.265625
IB18	72.50	0.238095238	0	0
IB19	73.00	0.421052632	0	0
IB20	112.00	0	0	
IB25	174.50	0	0	
IB26	177.00	0	0	
IB27	213.00	0	0	
IB28	213.50	0	0	
IB30	231.00	0	0	
IB33	253.00	0	0	
IB34	254.00	0	0	
IB35	309.50	0	0	
IB36	318.00	0	0	
IB38	363.00	0	0	
IB39	370.00	0	0.233796296	
IB41	395.00			1.346153846
IB44	420.00			1.818181818
IB47	430.00	0.388888889	0.777777778	2
IB51	441.00	0	0	
IB55	465.00			1.454545455
IB58	466.50	0	0	
IB60	477.00	0.305555556	0	0
IB63	485.00	0	0.346153846	

IB67	490.00	0.413793103	1.163793103	2.8125
IB70	498.00	0	0	
IB74	509.00	0	0	
IB77	520.00	0	0	
IB81	537.50	0	0	
IB84	548.00			2.3
IB85	553.50	0	0	
IB87	557.00	0	0	
IB89	562.50	0.386666667	0	0
IB93	582.50			1.5
IB96	588.50	0.463709677	0.423387097	0.913043478
IB99	593.00	0.375	0	0
IB102	611.50	0.428571429	0.321428571	0.75
IB106	619.50	0.392857143	0.5	1.272727273
IB107	632.00	0.923076923	0.884615385	0.958333333
IB109	645.50	0.446428571	0.513392857	1.15
IB114	661.50	0.4	0.818181818	2.045454545
IB118	682.00			1.636363636
IB120	687.00	0.45	0.520833333	1.157407407
IB126	744.50	0.328947368	0.381578947	1.16
IB127	759.00	0	0.390625	

Index Proxies

X-Ray Fluorescence: Representative mudstone and silty mudstone samples were analyzed for major and trace element abundances using a Bruker AXS TRACER III-V energy-dispersive hand-held X-ray fluorescence (XRF) unit (Bruker, Billerica, MA, USA) in the RED Lab at the University of Utah. Relative elemental abundances of each sample were measured for 180 seconds at 15 kV and 25 μ A for low mass major elements (Na, Mg, Al, Si, K, Ca) and 40 kV and 30 μ A for heavy trace elements (Ba, Sr) using XRF Core Scanner Control & Data Collection System software (DeWitt Systems, Inc., North Augusta, SC, USA). Helium was used for measurements of major elements, and a yellow Bruker filter composed of 12 mm Al and 1 mm Ti was used for measurements of trace elements. Raw data were collected as a spectrogram and converted to weight percent for major elements and ppm for trace elements using a matrix-specific mudstone calibration (Rowe et al., 2012).

Ischigualasto major and trace element proxies

CIA molar estimates range from 0.967 and 4.061, with medium values with low dispersion (1.487 to 2.465) in the first ~380 m and above ~600 m in section, and variable values and a high dispersion (0.967 to 4.061) between ~380 m and 600 m (Figure 2; Table S4). The K/Al ratio varies between 0.064 to 0.490, showing higher values with low dispersion (0.304 to 0.490) in the lower section (below ~380 m) and more variable values with high dispersion (0.064 - 0.468) above ~380 m in section (Figure 2; Table S4). The Ba/Sr ratio recorded values between 0.018 to 3.055, with high values dispersion in the lower section (until 380 m) and lower values and dispersion in the upper part of the section (Figure 2; Table S4).

Table S4. Index Proxies. The molar chemical index of alteration (CIA molar), K/Al, Ba/Sr were calculated based on X-ray fluorescence (XRF) mudstone facies of the Ischigualasto Formation at the Cerro Bola locality, Ischigualasto-Villa Union Basin, Argentina. The CIA molar is a sensitive measure of the degree of chemical weathering, the K/Al ratio reflects the chemical weathering intensity, and the Ba/Sr ratio is considered related to leaching intensity.

Sample	Section (m)	Na	Al	K	Ca	Ba	Sr	CIA molar	K/Al	Ba/Sr
IB2	2	0.0322685	0.0829972	0.0292937	0.0038147	17.916588	0.3456817	1.8998422	0.3529486	0.5916635
IB5	10.5	0.1694095	0.0796981	0.0325666	0.0054697	15.419529	0.5806681	1.7093682	0.4086241	0.3031371
IB7	21.5	0.3468861	0.0901622	0.0295623	0.004138	14.559002	-0.031978	1.8322892	0.3278788	
IB10	33.5	0.5404969	0.0636962	0.0200245	0.0040584	13.842346	0.2730653	1.9721983	0.3143746	0.5786809
IB11	36.5	0.5888996	0.0867024	0.0263921	0.0040308	17.076321	0.3093405	2.1676474	0.3043988	0.6301637
IB14	38.5	0.6211681	0.0774729	0.0300474	0.0035419	19.333309	0.4452354	1.7448292	0.3878442	0.4956926
IB16	43	0.6937722	0.0795393	0.0377514	0.0044423	18.013736	0.5684536	1.5800614	0.4746265	0.3617468
IB17	43.5	0.7018393	0.1041219	0.0368439	0.0057003	18.93739	0.4779652	2.0177833	0.3538535	0.4522929
IB18	71.5	1.1535979	0.084353	0.0361446	0.0043709	19.212195	0.7088699	1.7749972	0.4284916	0.30939
IB19	73	1.1777993	0.0744039	0.0246444	0.0036166	28.849782	2.4594867	1.8843552	0.3312246	0.1339041
IB20	112	1.8070345	0.0561504	0.0233785	0.0043448	12.559634	0.3759187	1.5457341	0.416354	0.3813985
IB25	173.5	2.7992901	0.0786697	0.0364173	0.0050994	18.147181	0.5107341	1.5656635	0.4629135	0.4056114
IB26	177.5	2.863827	0.0789703	0.0387682	0.0050395	19.205619	0.451846	1.5177097	0.4909207	0.4852145
IB27	213.5	3.4446596	0.0785348	0.0380862	0.0056578	19.109999	0.3277806	1.5012036	0.4849599	0.6655388
IB28	214.5	3.4607938	0.0790466	0.0317991	0.0052662	20.875724	0.4555965	1.6896915	0.4022825	0.5230667

IB30	231.5	3.7350758	0.0832323	0.0373933	0.0046584	17.649526	0.4122024	1.6829762	0.4492641	0.4887856
IB33	253	4.0819619	0.088593	0.0412511	0.0053653	17.10045	0.3911678	1.6431901	0.4656251	0.4990457
IB34	254	4.0980962	0.0724301	0.0289783	0.0069818	19.77996	1.2517317	1.6790439	0.4000866	0.180389
IB35	309.5	4.9935463	0.0869803	0.0370664	0.0047637	21.018555	0.5103398	1.7415317	0.4261465	0.4701531
IB36	319	5.1468216	0.060091	0.0208379	0.0036743	12.852601	0.7538901	1.7649235	0.3467716	0.1946162
IB38	363.5	5.8647951	0.0829431	0.0326131	0.008765	19.896298	1.8726108	1.6914934	0.3931985	0.1212888
IB39	370	5.9696676	0.0847721	0.0380046	0.0060576	20.236448	0.7920471	1.6183597	0.4483145	0.2916615
IB41	397	6.405292	0.0231853	0.001484	0.002019	3.0277568	1.8248084	0.967163	0.0640063	0.0189409
IB44	420	6.7763795	0.0807975	0.0165562	0.0054168	16.255813	1.1139437	2.7974418	0.2049094	0.1665871
IB47	430.5	6.945789	0.0969353	0.0257148	0.0055742	21.366477	0.7491738	2.3914835	0.265278	0.3255714
IB50	439	7.08293	0.0888286	0.0410029	0.0051473	21.993387	0.7898114	1.5903247	0.4615952	0.317881
IB51	442	7.1313327	0.0834736	0.0373742	0.0051686	18.249695	0.7524321	1.6441172	0.4477371	0.2768753
IB55	465.5	7.5104873	0.0891128	0.0128157	0.004809	8.0043772	0.3630639	3.3772434	0.1438148	0.2516752
IB58	466.5	7.5266215	0.0692136	0.0324045	0.0061392	14.138622	0.8666381	1.462088	0.4681816	0.1862367
IB64	487	7.8573733	0.0772558	0.0345357	0.0056757	15.059092	0.8093026	1.564133	0.4470307	0.2124143
IB67	491	7.9219103	0.0903327	0.0162346	0.0033194	14.482082	0.0541023	3.1001419	0.1797197	3.0557034
IB68	495	7.9864472	0.0517815	0.0150793	0.0032795	10.922703	0.8675405	1.6085864	0.29121	0.1437263
IB74	509	8.2123266	0.0453588	0.0141197	0.0028383	15.225817	1.0923365	1.383195	0.3112896	0.1591183
IB77	520	8.3898032	0.0618985	0.0242566	0.0061507	13.516377	1.4774712	1.4870245	0.3918773	0.1044329
IB81	537.5	8.6721523	0.0835915	0.0277999	0.0089335	17.325779	1.1721088	1.7959947	0.3325679	0.168741
IB84	547.5	8.8334947	0.0863482	0.0104477	0.0048387	5.804594	1.115715	3.4040255	0.1209947	0.0593902
IB85	553.5	8.9303001	0.0741273	0.0240033	0.0063519	16.517404	0.5673286	1.7600016	0.3238125	0.3323556
IB87	557	8.9867699	0.0575741	0.0226428	0.0036246	13.837205	0.9397646	1.5612693	0.3932814	0.1680835
IB89	562.5	9.0755082	0.0692415	0.0222464	0.0042808	14.960565	1.0750143	1.6835503	0.3212875	0.1588655
IB93	583	9.4062601	0.1153276	0.0104768	0.008808	8.7170058	1.7407183	4.0615083	0.0908436	0.0571656
IB96	588.5	9.4949984	0.0737213	0.0218269	0.0107187	13.689433	0.9556916	1.8057017	0.2960735	0.1635173
IB99	593	9.5676025	0.0728901	0.0273909	0.0114084	14.692854	0.8877731	1.4872491	0.3757834	0.1889296
IB102	611.5	9.8660858	0.064046	0.0200407	0.0113371	28.924662	3.891623	1.5595146	0.3129108	0.0848464
IB106	619.5	9.9951597	0.0781939	0.0255895	0.0062377	15.615313	0.6411466	1.8893643	0.3272578	0.2780284
IB107	632	10.196838	0.0682295	0.0210065	0.0177316	21.053775	1.1529281	1.4820116	0.3078802	0.2084604
IB111	650	10.487254	0.0527024	0.0138897	0.004711	15.455705	1.030793	2.2767986	0.2635493	0.1711643
IB114	661	10.664731	0.0830514	0.0243929	0.0085517	16.963278	1.2064718	1.9464362	0.2937088	0.160505
IB118	682	11.00355	0.1118443	0.0161375	0.0185035	69.149659	3.9710794	2.4658326	0.1442854	0.1987821
IB123	708	11.42304	0.0765713	0.0186009	0.0064293	17.287955	0.7199271	2.3963628	0.2429221	0.2741265
IB127	759	12.245886	0.0708455	0.0196765	0.0070675	13.265391	0.7321319	2.0717914	0.2777387	0.2068362

Climate variables

Table S5. Climate variables were calculated based on major and trace element abundances analyzed with X-ray fluorescence (XRF) on mudstone and silty mudstone facies of the Ischigualasto Formation at the Cerro Bola locality, Ischigualasto–Villa Union Basin, Argentina. The MAP ($(\Sigma \text{Base}/\text{Al})$) was used on the Ischigualasto levels interpreted as protocol, MAP (CALMAG) was applied to the Ischigualasto levels interpreted as vertisol and calcisols, MAT (PWI) was used on the Ischigualasto well-developed Bt horizon with mottled, and MAT (Al/Si) was used on the Ischigualasto levels that show incipient paleosol features.

Sample	Section (m)	MAP mm/yr ($\Sigma \text{Base}/\text{Al}$)	MAP mm/yr (CALMAG)	MAT °C (PWI)	MAT °C (Al/Si)
IB2	2				
IB5	10.5	758.1733878			10.89349719
IB7	21.5				
IB10	33.5				
IB11	36.5	814.3968165			13.29728503
IB14	38.5		1049.1298993	12.24842774	
IB16	43		944.7619245	11.80910458	
IB17	43.5		1212.867652	11.98604334	
IB18	71.5		1259.697717	12.27211309	
IB19	73		1343.522551	12.93212707	
IB20	112				
IB25	173.5		1019.406512	11.9506546	
IB26	177.5	721.0089442			13.01837114
IB27	213.5		956.9829422	11.79948953	
IB28	214.5		1029.727579	12.15446472	
IB30	231.5		950.1977268	11.82543403	
IB33	253	724.93465			14.1452913
IB34	254	740.3559513			12.49067397
IB35	309.5				
IB36	319		1174.012376	13.21243128	
IB38	363.5	752.4614482			13.36481113
IB39	370		1053.978697	11.88147032	
IB41	397				
IB44	420	846.2670928			13.80187325
IB47	430.5				
IB50	439	731.3194153			14.8689044
IB51	442		998.7498969	11.85791181	
IB55	465.5		1121.16245	13.51142085	
IB58	466.5		981.5033859	12.18354124	
IB64	487		1041.139046	12.06273141	
IB67	491				
IB68	495	821.2028566			13.49122253
IB74	509	828.8093588			13.80230176
IB77	520	742.4050433			9.41095332
IB81	537.5	785.5617687			13.4728555
IB84	547.5				
IB85	553.5		1127.685271	12.67774598	

IB87	557		1203.098381	13.07215699	
IB89	562.5	784.9634777			13.14468665
IB93	583				
IB96	588.5		1015.04599	12.8119567	
IB99	593		938.753844	12.28122393	
IB102	611.5		1077.997376	13.05867017	
IB106	619.5		1083.164823	12.58742608	
IB107	632	739.991216			13.64613063
IB111	650	1012.363756			10.52787509
IB114	661		1077.781818	12.59097039	
IB118	682	831.0587855			17.52850359
IB123	708		1274.742363	13.52991838	
IB127	759	790.0415048			10.99934838

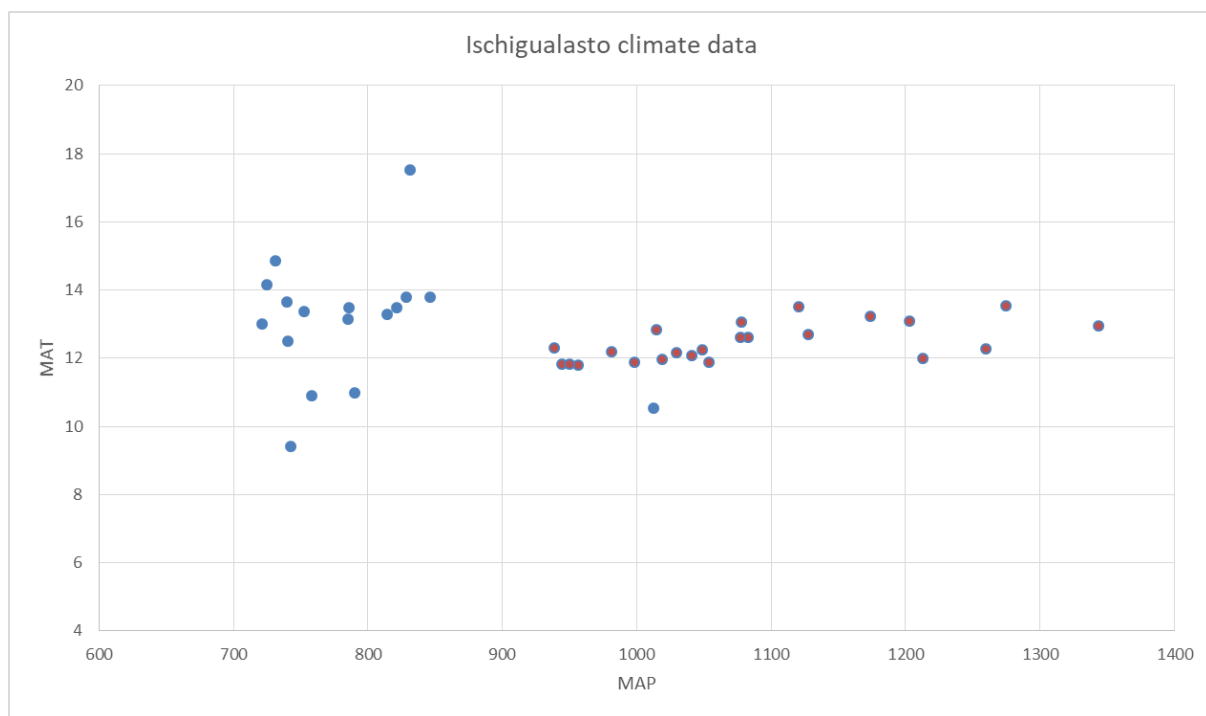


Figure S1. MAP and MAT dispersion graph of the Ischigualasto data according to different kinds of paleosols recorded (Blue dot: protocol, Red dot: vertisol and calcisols). The characteristic of each equation reduces the over-and under-estimate paleoprecipitation and paleotemperature but produces an artificial discontinuity.

Paleobotany record

The fossil plant content of the Ischigualasto-Villa Unión Basin has been studied by several authors, and these contributions have documented both plant macrofossils (Frenguelli, 1942, 1942b, 1942c, 1942d, 1943, 1944a, 1944b, 1944c, 1944d, 1944e, 1948; Groeber and Stipanicic, 1953; Archangelsky and Brett, 1961, 1963 Stipanicic, 1969, 1983; Stipanicic and Bonaparte, 1972, 1979; Colombi and Parrish, 2008; Mancuso, 2009; Arce and Lutz, 2010, 2014; Lutz et al., 2011) and microfossils (Herbst, 1965, 1970, 1972; Yrigoyen and Stolver, 1970; Ottone et al., 2005; Ottone and Mancuso, 2006; Césari and Colombi, 2013; Perez Lonaize et al., 2018).

The Agua de la Peña Group recorded rich micro, and macrofossil plant remains (Table S6, S7). In the Chañares Formation, there is no register of macrofossil plant remains. The palynological assemblages of the Chañares Formation (Table S7) are dominated by bisaccate pollen grains (*Alisporites*, *Platysaccus*). In less proportion, striate pollen grains and fern spores, characteristic of the Ipswich Subprovince (Dolby and Blame, 1976), also were recorded taxa such us *Ovalipollis* and *Ellipsovelatisporites*, that are characteristic elements of the Onslow Subprovince (Perez Loinaze et al., 2018).

The fossil flora of the Los Rastros Formation includes the following taxa (Table S6): Equisetopsida (*Equisetites*, *Neocalamites*, *Phyllotheeca*), Polypodiopsida (*Cladophlebis*), Umkomasiales (*Dicroidium*, *Johstonia*, *Xylopteris*, *Rhexoxylon*, *Zuberia*), Peltaspermales (*Pachydermophyllum*), Petriellales (*Rochipteris*), Ginkgoales (*Baiera*, *Sphenobaiera*), Voltziales (*Heidiphyllum*), Coniferales (*Rissikia*), Gnetales (*Yabearella*) and uncertain affinity Gymnosperms (*Dejerseya*, *Kurtziana*, *Dordrectites*) (Frenguelli, 1942, 1943, 1944, 1946, 1947, 1948; Groeber and Stipanicic, 1953; Zamuner et al., 2001; Stipanicic and Marsicano, 2002; Mancuso et al., 2009; Arce and Lutz, 2010, 2014; Lutz et al., 2011; Pedernera et al., 2020; Beltrán et al., 2021). The microfossil associations of the Los Rastros Formation (Table S7) are characterized by the presence of bisaccate pollen grains assigned to Umkomasiales/Peltaspermales (*Alisporites*), abundant inaperturate and diploxylonoid bisaccate pollen grains of Coniferales affinity (e.g., *Inaperturapollenites*, *Platysaccus*, *Cedripites*), together with monosulcate pollen assigned to Cycadales/Bennettitales/Ginkgoales or Pentoxylales (*Cycadopites*), and other saccate forms of uncertain affinity (*Variapollenites*), and spores of terrestrial plants (*Cadargasporites*, *Leptolepidites*, *Osmundacidites*, *Aratrisporites*, *Calamospora*), and freshwater algae (*Botryococcus* and *Plaesiodictyon*). (Herbst, 1970, 1972; Zavattieri and Melchor, 1999; Ottone et al., 2005; Ottone and Mancuso, 2006). The palynoflora of the Los Rastros resembles the cool temperate Ipswich microflora (Dolby and Balme, 1976).

The Ischigualasto Formation fossil plant association (Table S6) includes Equisetopsida (*Neocalamites*), Polypodiopsida (*Cladophlebis*), Umkomasiales (*Dicroidium*, *Johstonia*, *Xylopteris*, *Zuberia*), Peltaspermales (*Scytophyllum*), Ginkgoales (*Ginkgoites*), Voltziales (*Heidiphyllum*), Coniferales (*Araucarioxylon*, *Protojuniperoxylon*), Gnetales (*Yabearella*) (Archangelsky, 1968; Zamuner et al., 2001; Stipanicic and Marsicano, 2002; Colombi and Parrish, 2008; Drovandi et al., 2021). The microfloral associations of the Ischigualasto Formation are characterized by the dominance of bisaccate pollen grains (*Alisporites*, *Falcisporites*) and monosulcate pollen (*Cycadopites*) are also common. The Ischigualasto palynofloras also include typical taxa of Onslow palynofloras (Rogers et al., 1993; Martínez et al., 2011; Césari and Colombi, 2013, 2016).

The paleobotanical record of the Los Colorados Formation (Table S6) is scarce and limited to the presence of permineralized trunks of *Rhexoxylon* (Umkomasiales) and *Araucarites* (Coniferales) and impressions of fronds assigned to *Cladophlebis* (Bonaparte, 1997). There is no register of palynological assemblages in the Los Colorados Formation.

Table S6. Plant macrofossil record of formations from the Agua de la Peña Group. Data from references are listed in Table S9.

Taxonomic groups	Taxa	Los Rastros Fm.	Ischigualasto Fm.	Los Colorados Fm.
Lycopsida	<i>Pleuromeia</i> sp.	X		
Equisetopsida	<i>Equisetites fertilis</i>	X		
	<i>Neocalamites carrerei</i>	X	X	
	<i>Neocalamites ischigualasti</i>	X		
	<i>Neocalamites ramaccionii</i>	X		
	<i>Neocalamites</i> sp.	X		
	<i>Nododendron</i> sp.	X		
	<i>Phyllotheca australis</i>	X		
Polypodiopsida	<i>Cladophlebis mendozaensis</i>	X	X	
	<i>Cladophlebis mesozoica</i>	X		
	<i>Cladophlebis</i> sp. cf. <i>C. mesozoica</i>	X		
	<i>Cladophlebis</i> sp.			X
Umkomasiales	<i>Dicroidium dubium</i>	X		
	<i>Dicroidium nondichotoma</i>	X		
	<i>Dicroidium obtusifolium</i>	X		
	<i>Dicroidium odontopteroides</i>	X	X	
	<i>Dicroidium argenteum</i>	X		
	<i>Dicroidium crassum</i>	X		
	<i>Dicroidium lancifolium</i>	X	X	
	<i>Dicroidium lineatum</i>	X		
	<i>Johnstonia coriacea</i>	X	X	
	<i>Johnstonia dutoiti</i>	X		
	<i>Johnstonia stelzneriana</i>	X	X	
	<i>Matatiella rosetta</i>	X		
	<i>Rhexoxylon piatnitzkyi</i> **		X	
	<i>Rhexoxylon</i> sp. **	X		X
	<i>Umkomasia</i> sp.*	X		
	<i>Xylopteris argentina</i>	X	X	
	<i>Xylopteris densifolia</i>	X		
	<i>Xylopteris elongata</i>	X	X	
	<i>Xylopteris rigida</i>	X		
	<i>Zuberia brownii</i>	X		
	<i>Zuberia feistmantelii</i>	X		
	<i>Zuberia papillata</i>		X	
	<i>Zuberia sahini</i>	X	X	
	<i>Zuberia zuberi</i>	X	X	
Peltaspermales	<i>Lepidopteris stormbergensis</i>		X	

	<i>Pachydermophyllum papillosum</i>	X		
	<i>Pachydermophyllum praecordillerae</i>	X		
	<i>Peltaspermum monodiscum</i> *	X		
	<i>Scytophyllum neuburgianum</i>		X	
Petriales	<i>Rochipteris alexandriana</i>	X		
Cycadales and Bennettiales	<i>Kurtziana cacheutensis</i>	X		
	<i>Michelilloa waltonii</i>		X	
	<i>Pterophyllum</i> sp.		X	
	<i>Taeniopteris</i> sp.		X	
Ginkgoales	<i>Baiera (=Sphenobaiera) africana</i>	X		
	<i>Baiera (=Sphenobaiera) pontifolia</i>	X		
	<i>Baiera (=Sphenobaiera) schenkii</i>	X		
	<i>Ginkgoites</i> sp.		X	
	<i>Sphenobaiera argentiniae</i>	X		
	<i>Sphenobaiera insecta</i>	X		
	<i>Sphenobaiera sectina</i>	X		
Czekanowskiales	<i>Czekanowskia rigali</i>	X		
	<i>Czekanowskia</i> sp.	X		
Voltziales	<i>Cycadocarpium andium</i> *	X		
	<i>Heidiphyllum clarifolium</i>	X		
	<i>Heidiphyllum elongatum</i>	X	X	
	<i>Heidiphyllum minutifolium</i>	X		
	<i>Heidiphyllum</i> sp.	X		
	<i>Telemachus elongatus</i> *	X		
	<i>Telemachus</i> sp. *	X		
Coniferales	<i>Araucarioxylon</i> sp. **		X	
	<i>Araucarites</i> sp.**			X
	<i>Protojuniperoxylon ischigualensis</i> **		X	
	<i>Rissikia media</i>	X		
Uncertain affinity Gymnosperms	<i>Acevedoa rastroensis</i> *	X		
	<i>Cordaicarpus</i> sp.*	X		
	<i>Dejerseya lobata</i>	X		
	<i>Dejerseya lunensis</i>	X		
	<i>Desmiophyllum</i> sp.	X		
	<i>Dordrectites elongatus</i> *	X		
	<i>Dordrectites</i> sp. *	X		
	<i>Harringtonia argentinica</i>	X		
	<i>Pelourdea polyphylla</i>	X		

	<i>Pelourdea problematica</i>	X		
	<i>Pelourdea</i> sp.	X		
	<i>Phoenicopsis</i> sp.	X		
	<i>Pterorrhachis ambigua</i>	X		
	<i>Samaropsis</i> sp.*	X		
	<i>Sphenopteris</i> sp.	X		
Gnetales	<i>Yabeiella brackebuschiana</i>	X	X	
	<i>Yabeiella mareyesiaca</i>	X	X	
	<i>Yabeiella</i> sp.		X	
	<i>Yabeiella spathulata</i>	X		

Table S7. Miospores record of formations from the Agua de la Peña Group. Data from references are listed in Table S9.

SPORES	Chañares Fm.	Los Rastros Fm.	Ischigualasto Fm.
<i>Annulispora folliculosa</i>			X
<i>Apiculatisporis</i> sp. cf. <i>A. argentinus</i>		X	
<i>Baculatisporites comaumensis</i>		X	
<i>Baculatisporites</i> sp. cf. <i>B. comaumensis</i>		X	
<i>Birerisporites</i> sp.		X	
<i>Cacheutasporites minutus</i>		X	
<i>Cadargasporites baculatus</i>		X	X
<i>Cadargasporites</i> cf. <i>baculatus</i>		X	
<i>Cadargasporites</i> cf. <i>verrucosus</i>		X	
<i>Cadargasporites cuyanensis</i>		X	
<i>Cadargasporites granulatus</i>			X
<i>Cadargasporites reticulatus</i>			X
<i>Cadargasporites senectus</i>	X		X
<i>Cadargasporites</i> cf. <i>granulatus</i>		X	
<i>Calamospora impexa</i>		X	
<i>Calamospora</i> spp.		X	X
<i>Calamospora tener</i>		X	
<i>Carnisporites anteriscus</i>			X
cf. <i>Carnisporites megaspiniger</i>			X
cf. <i>Craterisporites</i> sp.		X	
cf. <i>Kraeuselisporites punctatus</i>		X	
cf. <i>Osmundacidites cacheutensis</i>		X	
cf. <i>Pustulatisporites blackstonensis</i>		X	
<i>Cingutriletes</i> sp.		X	
<i>Cingutriletes</i> sp.			X
<i>Cingutriletes</i> sp. cf. <i>C. cestus</i>			X
<i>Cirratirradites</i> sp.		X	
<i>Clavatisporites conspicuus</i>		X	X
<i>Clavatisporites</i> sp.		X	
<i>Clavatisporites</i> sp. cf. <i>C. conspicuus</i>		X	
<i>Clavatriletes dubius</i>		X	
<i>Con verrucosporites cameronii</i>		X	
<i>Con verrucosporites</i> sp.		X	
<i>Cyathidites minor</i>	X		
<i>Cyathidites australiensis</i>	X		
<i>Cyclogranisporites</i> sp.		X	

<i>Deltoispora</i> sp. a		X	
<i>Deltoispora</i> sp. b		X	
<i>Deltoispora</i> sp. c		X	
<i>Densoisporites</i> sp. cf. <i>D. complicatus</i>		X	
<i>Densosiporites psilatus</i>		X	
<i>Dictyophyllidites harrisii</i>		X	X
<i>Dictyophyllidites mortonii</i>		X	X
<i>Foveosporites mimosae</i>			X
<i>Granasporites erdtmanii</i>		X	
<i>Granulatisporites</i> sp.		X	
<i>Inapertisporites</i> sp.		X	
<i>Interulobites</i> sp.	X		
<i>Leiotriletes directus</i>		X	
<i>Leptolepidites argenteaeformis</i>	X		X
<i>Leptolepidites bossus</i>		X	
<i>Leptolepidites crassibalteus</i>		X	
<i>Leptolepidites lobatoverrucosus</i>		X	
<i>Leptolepidites</i> sp.		X	
<i>Leptolepidites</i> sp. cf. <i>L. crassibalteus</i>		X	X
<i>Leptolopidites</i> sp. cf. <i>L. argenteaeformis</i>		X	
<i>Limatulasporites fossulatus/limatulus complex</i>	X		X
<i>Lophotriletes bauhiniae</i>			X
<i>Lophotriletes</i> sp. cf. <i>L. bauhiniane</i>		X	
<i>Lundbladispora punctata</i>			X
<i>Lundbladispora</i> sp.			X
<i>Lundbladispora stellae</i>		X	
<i>Lundblandispora</i> spp.		X	
<i>Lycospora</i> sp. cf. <i>L. salebrocea</i>		X	
<i>Neoraistrickia</i> sp.		X	
<i>Osmundacidites parvus</i>		X	
<i>Osmundacidites wellmanii</i>		X	X
<i>Osmundacidites bonapartei</i>		X	
<i>Osmundacidites burguerii</i>		X	
<i>Osmundacidites senectus</i>		X	
<i>Osmundacidites fissus</i>			X
<i>Osmundacidites</i> sp.			X
<i>Osmundacidites</i> spp.		X	
<i>Paraconcavisporites</i> sp.		X	
<i>Perisporate</i> spore indet	X		
<i>Playfordiaspora cancellosa</i>	X	X	X

<i>Polypodiidites mutabilis</i>			X
<i>Polypodiisporonites (ex Thymospora) ipsviciensis</i>		X	
<i>Psilomonoporites sp. cf. P. cacheutensis</i>		X	
<i>Psilomonoporites balmei</i>		X	
<i>Punctatisporites</i> spp.		X	
<i>Raistrikia ramosa</i>		X	
<i>Regulatisporites nelsonensis</i>		X	
<i>Regulatisporites</i> sp.		X	
<i>Retitriletes</i> sp.			X
<i>Retusotriletes herbstii</i>			X
<i>Retusotriletes wielandii</i>		X	
<i>Rogalskaisporites cicatricosus</i>			X
<i>Rugulatisporites permixtus</i>	X	X	X
<i>Rugulatisporites</i> sp. cf. <i>R. neuquenensis</i>			X
<i>Secarisporites volkheimeri</i>		X	
Spore indet 1	X		
Spore indet 2	X		
Spore indet 3	X		
<i>Stereisporites neuquenensis</i>		X	
<i>Stereisporites</i> sp. cf. <i>S. psilatus</i>		X	
<i>Stereisporites</i> spp.		X	
<i>Striatella seebergensis</i>			X
<i>Striatiti</i> spp.		X	
<i>Taurocusporites</i> sp. A			X
<i>Uvaesporites glomeratus</i>		X	X
<i>Uvaesporites hammenii</i>		X	X
<i>Uvaesporites verrucosus</i>		X	X
<i>Uvaesporites</i> sp.		X	
<i>Verrucosisporites riojanus</i>		X	
<i>Verrucosisporites archangelsky</i>		X	
<i>Verrucosisporites</i> sp. a		X	
<i>Verrucosisporites</i> sp. b		X	
<i>Verrucosisporites</i> spp.		X	
POLLEN			
' <i>Rimaesporites</i> ' <i>aqulonalis</i>			X
<i>Abnormal pollen grains</i>			X
<i>Accinctisporites cacheutensis</i>		X	
<i>Accinctisporites circumdatus</i>		X	
<i>Accinctisporites excentricus</i>		X	

<i>Accinctisporites grandior</i>		X	
<i>Accinctisporites ligatus</i>		X	
<i>Accinctisporites sinuosus</i>		X	
<i>Alisporites argentinus</i>		X	
<i>Alisporites australis</i>	X	X	X
<i>Alisporites cacheutensis</i>		X	
<i>Alisporites grandis</i>		X	
<i>Alisporites indicus</i>		X	
<i>Alisporites lowoodensis</i>		X	
<i>Alisporites ovatus</i>		X	
<i>Alisporites parvus</i>	X	X	X
<i>Alisporites plicatus</i>	X		
<i>Alisporites similaris (similis)</i>	X	X	
<i>Alisporites sp. cf. A. landianus</i>		X	
<i>Alisporites sp. cf. A. tenuicorpus</i>	X		
<i>Alisporites spp.</i>		X	X
<i>Alisporites sulcatus</i>	X		X
<i>Anapiculatisporites cf. pamelae</i>		X	
<i>Anapiculatisporites cooksonae</i>			X
<i>Anapiculatisporites sandrae</i>		X	X
<i>Anapiculatisporites sp. cf. A. pristidentatus</i>		X	
<i>Anapiculatisporites spiniger</i>			X
<i>Aratrisporites compositus</i>		X	
<i>Aratrisporites parvispinosus</i>			X
<i>Aratrisporites sp. cf. A. flexibilis</i>		X	
<i>Aratrisporites sp. cf. A. parvinosus</i>		X	
<i>Aratrisporites sp. cf. A. wollariensis</i>		X	
<i>Araucariacites australis</i>		X	X
<i>Araucariacites sp. cf. A. pergranulatus</i>		X	
<i>Ashmoripollis sp.</i>			X
<i>Brachysaccus eskensis</i>		X	
<i>Brachysaccus sp.</i>			X
<i>Brachysaccus sp. A</i>		X	
<i>Cedripites pannellai</i>		X	
<i>Cedripites priscus</i>		X	
<i>Cedripites sp. cf. C. pannellai</i>		X	
<i>Cedripites sp. cf. C. priscus</i>		X	
<i>Cedripites tectus</i>		X	
<i>cf. Callialasporites dampieri</i>			X
<i>cf. Cuneatisporites radialis</i>		X	

<i>cf. Dacrycarpites sp.</i>		X	
<i>cf. Densipollenites indicus</i>		X	
<i>cf. Densipollenites densus</i>		X	
<i>cf. Duplicisporites verrucosus</i>		X	
<i>cf. Duplicisporites granulatus</i>	X		
<i>cf. Vesicaspora cacheutensis</i>		X	
<i>cf. Vesicaspora jansoniusii</i>		X	
<i>Chordasporites singulichorda</i>			X
<i>Chordasporites australiensis</i>		X	
<i>Chordasporites spp.</i>			X
<i>Crustae sporites sp.</i>	X		
<i>Cycadopites enormis</i>		X	
<i>Cycadopites follicularis (nitidus)</i>		X	
<i>Cycadopites granulatus</i>			X
<i>Cycadopites magnus</i>		X	
<i>Cycadopites stonei</i>			X
<i>Cycadopites tivoliensis</i>		X	
<i>Cycadopites (Megamonoporites) argentinus</i>		X	
<i>Cycadopites (Monosulcites) balmei</i>		X	
<i>Cycadopites adjectus</i>		X	
<i>Cycadopites linae</i>		X	
<i>Cycadopites sp. A</i>		X	
<i>Cycadopites sp. cf. C. andrewsii</i>		X	
<i>Cycadopites sp. cf. C. follicularis</i>		X	
<i>Cycadopites sp. cf. C. granulatus</i>		X	
<i>Cycadopites spp.</i>		X	
<i>Cycadopites spp.</i>			X
<i>Ellipsovelatisporites plicatus</i>	X		X
<i>Ellipsovelatisporites spp.</i>			X
<i>Enzonatasporites vigens</i>			X
<i>Equisetosporites cacheutensis</i>		X	
<i>Equisetosporites sp. cf. E. tortuosus</i>			X
<i>Equisetosporites steevesii</i>			X
<i>Falcisporite spp.</i>			X
<i>Falcisporites nuthallensis</i>	X	X	X
<i>Falcisporites sp. cf. F. stabilis</i>		X	
<i>Falcisporites sp. cf. F. zapfei</i>			X
<i>Goubinispora morondavensis</i>		X	
<i>Granamonocolpites cacheutensis</i>		X	
<i>Granamonocolpites luisae</i>		X	
<i>Granomonocolpites blancae</i>		X	

<i>Inaperturopollenites nebulosus</i>		X	
<i>Inaperturopollenites reidii</i>		X	
<i>Inaperturopollenites</i> spp.		X	
<i>Indusiisporites parvisaccatus</i>		X	
<i>Klausipollenites argentinus</i>		X	
<i>Klausipollenites schaubergerii</i>		X	
<i>Klausipollenites staplinii</i>		X	
<i>Lueckisporites</i> sp. cf. <i>L. singhii</i>		X	X
<i>Lueckisporites</i> spp.		X	
<i>Lunatisporites noviaulensis</i>			X
<i>Lunatisporites</i> sp. cf. <i>L. noviaulensis</i>		X	
<i>Lunatisporites</i> spp.		X	X
<i>Megamonoporites cacheutensis</i>		X	
<i>Megamonoporites parvus</i>		X	
<i>Minutosaccus crenulatus</i>			X
<i>Minutosaccus</i> sp.			X
<i>Minutosacus</i> sp.		X	
<i>Monosulcites castroensis</i>		X	
<i>Monosulcites enormis</i>		X	
<i>Monosulcites minimus</i>		X	
<i>Monosulcites schizocolpatus</i>		X	
<i>Monosulcites</i> sp.		X	
<i>Monosulcites</i> sp. cf. <i>M. minimus</i>		X	
<i>Ovalipollis ovalis</i>	X		X
<i>Ovalipollis</i> spp.			X
<i>Ovallipoliis pseudoalatus</i>			X
<i>Parcisorites cacheutensis</i>		X	
<i>Parcisorites cirratus</i>		X	
<i>Parcisorites tenuis</i>		X	
<i>Partitisporites</i> spp.			X
<i>Patinasporites densus</i>			X
<i>Platysaccus leschikii</i>	X		
<i>Platysaccus queenslandi</i>	X	X	X
<i>Platysaccus papilionis</i>	X	X	
<i>Platysaccus rhombicus</i>		X	
<i>Platysaccus</i> sp. cf. <i>P. cacheutensis</i>		X	
<i>Platysaccus</i> sp. cf. <i>P. rhombicus</i>	X		
<i>Podocarpidites ellipticus</i>	X		
<i>Podocarpidites multesimus</i>	X		
<i>Podocarpidites</i> sp. cf. <i>P. dettmaniae</i>	X		
<i>Podocarpidites</i> sp. cf. <i>P. ellipticus</i>		X	

<i>Podocarpidites</i> spp.		X	
<i>Polysaccites</i> sp.		X	
<i>Protodiploxylinus</i> sp. cf. <i>P. schizeatus</i>		X	
<i>Protodiploxylinus</i> sp. cf. <i>P. ujhelyi</i>	X		
<i>Protohaploxylinus samoilovichii</i>			X
<i>Protohaploxylinus microcorpus</i>			X
<i>Protohaploxylinus</i> sp.		X	
<i>Protohaploxylinus</i> sp. cf. <i>hartii</i>			X
<i>Protohaploxylinus</i> sp. cf. <i>P. amplus</i>		X	
<i>Protohaploxylinus</i> sp. cf. <i>P. diagonalis</i>		X	
<i>Protohaploxylinus</i> sp. cf. <i>P. limpidus</i>		X	
<i>Protohaploxylinus</i> sp. cf. <i>P. microcorpus</i>		X	
<i>Protohaploxylinus</i> sp. cf. <i>P. varius</i>		X	
<i>Protohaploxylinus</i> spp.		X	
<i>Protohaplylinus hartii</i>	X		
<i>Pteruchopollenites</i> sp.			X
<i>Pteruchopollenites</i> spp.		X	
<i>Punctamonocolpites wielandii</i>		X	
<i>Quadraeculina anellaeformis</i>			X
<i>Rimaesporites</i> spp.			X
<i>Samaropollenites speciosus</i>			X
<i>Scheuringipollenites</i> sp. cf. <i>S. maximus</i>	X		
<i>Scutasporites unicus</i>	X		
<i>Spheripollenites cacheutensis</i>		X	
<i>Spheripollenites niger</i>		X	
<i>Spheripollenites stellarius</i>		X	
<i>Staurosaccites quadrifidus</i>			X
<i>Steevesipollenites claviger</i>		X	X
<i>Striatoabieites aytugii</i>	X		X
<i>Striatoabieites</i> sp. cf. <i>S. richteri</i>	X		
<i>Striatoabieites</i> spp.		X	
<i>Striatopodocarpidite</i> sp. cf. <i>S. communis</i>	X		
<i>Striatopodocarpidites pantii</i>	X	X	
<i>Striatopodocarpidites rarus</i>	X	X	
<i>Striatopodocarpidites</i> sp. 1	X		
<i>Striatopodocarpites</i> sp. 2		X	

<i>Sulcatisporites ovatus</i>		X	
<i>Sulcatisporites nilssoni</i>		X	
<i>Sulcatisporites</i> sp. cf. <i>S. institutus</i>		X	
<i>Sulcatisporites</i> sp. cf. <i>S. kraeuseli</i>		X	
<i>Sulcatisporites</i> sp. cf. <i>S. triassicus</i>		X	
<i>Sulcosaccispora alaticonformis</i>		X	
<i>Sulcosaccispora lata</i>		X	
<i>Tenuisaccites fragilis</i>		X	
<i>Triadispora plicata</i>			X
<i>Triadispora plicata</i>			X
<i>Triadispora</i> sp. cf. <i>T. crassa</i>	X		
<i>Triadispora</i> spp.			X
<i>Trisaccites</i> sp.		X	
<i>Vallasporites ignacii</i>	X		X
<i>Variapollenites curviplicatus</i>		X	
<i>Variapollenites rhombicus</i>		X	
<i>Variapollenites trisulcus</i>		X	
<i>Vesicaspora ovata</i>		X	
<i>Vitreisporites microsaccus</i>		X	
<i>Vitreisporites signatus</i>		X	
<i>Vitreisporites subtilis</i>		X	
<i>Vitreisporites pallidus</i>		X	
<i>Vitreisporites</i> sp. cf. <i>V. contextus</i>		X	
<i>Zonalasporites cinctus</i>			X
Freshwater alga			
<i>Botryococcus</i> sp.		X	
<i>Botryococcus</i> sp. cf. <i>B. braunii</i>			X
<i>Pilasporites crateriformis</i>		X	
<i>Pilasporites calculus</i>		X	
<i>Plaesiodyction mosellanicum</i> ssp. <i>perforatum</i> (?)		X	
<i>Plaesiodyction mosellanicum</i> ssp. <i>variabile</i> (?)		X	
<i>Schizosporis cooksonae</i>		X	

Stratigraphic distribution of plants through the sections and taphonomy

The absence of plant macrofossils in the Chañares Formation and palynomorphs preserved in concretions (Perez Lonaize et al., 2018) could be related to the low preservation potential of macroplant remains and the development of depositional environments with high oxidation conditions and low water tables (Gastaldo et al., 2005).

Regarding the distribution of plant macrofossils along the sequence, in the Los Rastros Formation in the Gualo Area, the number of taxa decreases towards the upper section of the unit. Otherwise, in the Agua de la Peña area (from the Los Rastros Formation), the number of registered taxa increases towards the top of the unit. Finally, in the Ischichuca area from the Los Rastros Formation, the highest number of taxa is recorded in the middle section of the unit (Pedernera et al., 2020). The plant remains are preserved mainly like compressions and impressions (Pedernera et al., 2020). The preservation of macrofossils in the Los Rastros Formation is similar throughout the column; no significant changes are observed in the style of preservation or in the type of remains that are preserved (Pedernera et al., 2021). Preservation of plant remains in proximal areas of the system (delta) would have been favored by rapid burial and high-water strand lines despite the oxygenation of the sediments. The development of anoxic bottom water and bed favored the preservation (Mancuso and Marsicano, 2008; Mancuso, 2009; Pedernera et al., 2020).

In the Ischigulasto Formation, the type of preservation and preserved plant remains varies throughout the unit (Colombi and Parrish, 2008). In the lower part of the unit (UI and UII) and the upper section (UIV), the plant remains are represented by root halos, root traces, and stumps and roots of shrubby plants. While in the middle part (UIII), plant remains are represented by a major number of preservation styles and types of remains, such as silicified trunks, cuticles debris, impressions, and charcoal fragments (Colombi and Parrish, 2008; Drovandi et al., 2021). The halo and trace roots would have been preserved due to the development of poorly drained paleosoils and high level of the water table. In contrast, preservation of silicified trunks, cuticles debris, impressions, and charcoal fragments preserved in abandoned channel facies could be enhanced by the high sedimentation rate (Colombi and Parrish, 2008; Drovandi et al., 2021).

In the case of the Los Colorados Formation, scarce materials reported and the lack of taphonomic complex difficult to interpret possible links between the plant paleocommunities and climatic parameters.

Climatic conditions can give rise to taphonomic biases; in arid conditions, the preservation potential is lower and restricted to sub-environments with particular humidity conditions. In conditions of higher humidity (e.g., high water table), preservation potential increases (Spicer, 1991; Behrensmeyer and Hook, 1992; Martin-Closas and Gómez, 2004; Gastaldo et al., 2005; Nowak et al., 2020). This could lead to erroneous interpretations of the paleoenvironmental and paleoclimatic characteristics of the sequences (e.g., Gastaldo et al. 2005).

Tetrapod record

The tetrapod record of the Agua de la Peña Group in the Ischigualasto-Villa Unión Basin has been studied since 1960 (e.g., Romer and Jensen 1966; Bonaparte, 1972, 1997; Rogers et al., 1993; Arcucci et al., 2004; Marsicano et al., 2007; Martinez et al., 2013; Mancuso et al., 2014; Desojo et al., 2020). The Agua de la Peña paleontological content is unequaled worldwide for its diverse and well-preserved Late Triassic tetrapod assemblages (Table S8). These include, among others, temnospondyl amphibians, one of the oldest turtles, non-mammalian therapsids, dinosaur precursors, ornithischian and theropod dinosaurs, and, probably, the oldest putative theropod trackways (e.g., Bonaparte, 1997; Rogers et al., 1993, 2001; Marsicano et al., 2007).

The early Carnian Chañares Formation (Marsicano et al., 2016) has a distinctive tetrapod assemblage, which includes a high taxonomic diversity of archosauriforms (e.g., proterochampsids, pseudosuchians, ornithodirans) and a high abundance of synapsids (large dicynodonts and small- to medium-sized cynodonts) (Table S8, S9). This assemblage records the origin and early diversification of dinosaurs and the dominance of therapsids.

The middle Carnian Los Rastros Formation (Mancuso et al., 2020) vertebrate fossil assemblage includes fragmentary body fossils of indeterminate temnospondyls (Mancuso and Marsicano, 2008). Diverse tetrapod tracks of therapsids, pseudosuchians, and dinosauromorphs (Marsicano et al., 2004, 2007, 2010) are also recorded at several sites in the area (Table S8, S9).

The late Carnian-early Norian Ischigualasto Formation (Martinez et al., 2011; Desojo et al., 2020; Colombi et al., 2021) preserves abundant and diverse vertebrate assemblage, including representatives of the two major dinosaur clades (Ornithischia and Saurischia), which already diversified, basal archosauromorphs (proterochampsids and rhynchosaurs), non-dinosaur dinosauromorphs, diverse crurotarsan archosaurs, carnivorous and herbivorous cynodonts, large dicynodonts, and amphibians (Table S8, S9)

Finally, the lower levels of the Norian Los Colorados Formation (Kent et al., 2014) records one of the youngest dicynodonts (*Jachaleria colorata*) of Gondwana. In contrast, in the upper levels, a diverse assemblage is preserved, with dinosaurs as dominant components of the ecosystem (Table S8, S9). While it includes high diversity of sauropodomorph and theropod taxa, basal and derived representatives of the crocodylian lineage, one of the oldest turtles, and non-mammaliaform cynodonts are scarcely represented (Table S8, S9).

The Ischigualasto Formation has the highest preserved species richness with 31 taxa, followed by the Los Colorados (21 taxa) and Chañares formations (20 taxa) (Figure S2; Table S8). The Los Rastros Formation preserves few body fossils but records a diverse assemblage of tetrapod footprints including therapsids, archosaurs, and dinosauromorphs (Marsicano et al., 2004, 2007, 2010). Therapsids (dicynodont and cynodont), pseudosuchians, and dinosauromorphs are recorded in all three formations, but with varying diversity (Figure S2; Table S8). In contrast, temnospondyls are recorded only in the Los Rastros and Ischigualasto formations, and rhynchosaurs and proterochampsids are recorded in the Chañares and Ischigualasto formations (Figure S2; Table S8). Finally, testudinatans (turtles) are exclusively recorded in the Los Colorados Formation (Figure S2; Table S8).

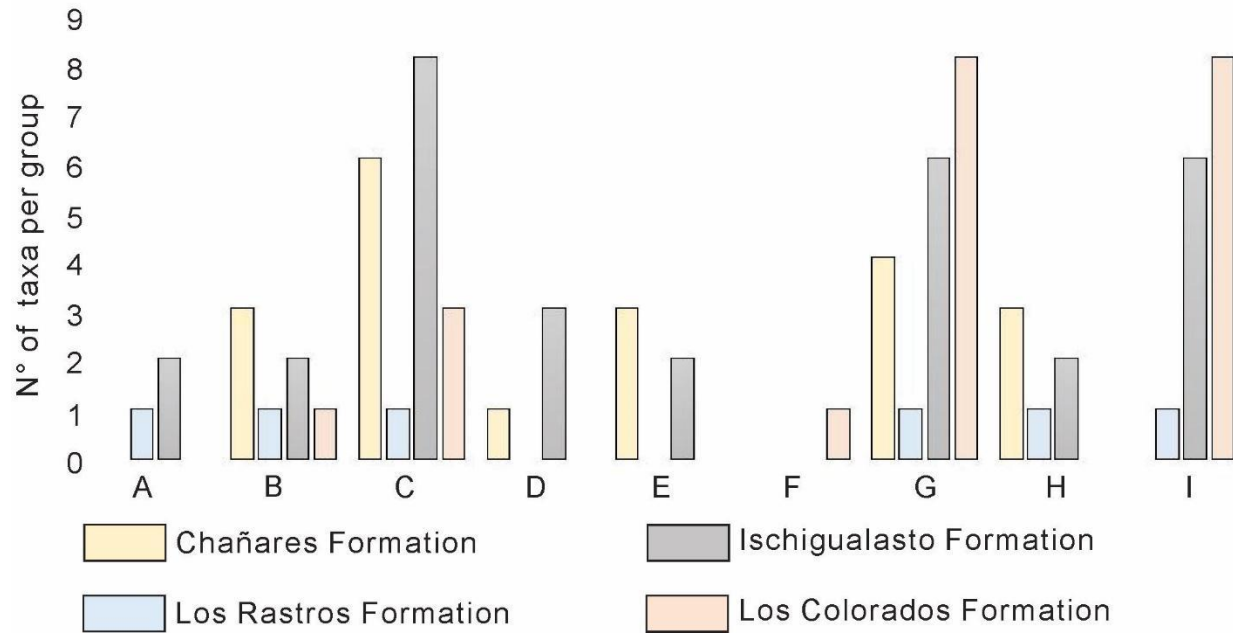


Figure S2. Paleovertebrate record in the units of the Agua de la Peña Group. Number of vertebrate taxa per taxonomic group in each unit. A. Temnospondyli, B. Dicynodontia, C. Cynodontia, D. Rhynchosauria, E. Proterochampsidae, F. Testudinata, G. Pseudosuchia, H. Early Dinosauromorpha, I. Dinosauria.

Tables S8. Tetrapod taxa record of the different Agua de la Peña Group units, the Ischigualasto-Villa Unión Basin. Data from references are listed in Table S9.

Taxonomic group	Taxa	Chañares Fm.	Los Rastros Fm.	Ischigualasto Fm.	Los Colorados Fm.
Temnospondyli	<i>Temnospondil</i> indet.		x		
	<i>Pelorocephalus</i>			x	
	<i>Promastodonsaurus</i>			x	
Dicynodontia	Dicynodont indet.	x	x		
	<i>Dinodontosaurus</i>	x			
	<i>Stahleckeria</i>	x			
	<i>Ischigualastia</i>			x	
	<i>Jachaleria</i>			x	x
Cynodontia	Cynodont indet.	x	x	x	
	<i>Massetognathus</i>	x			
	<i>Scalenodon/Mandagomphodon</i>	x			
	<i>Chiniquodon t.</i>	x			
	<i>Probainognathus</i>	x			
	<i>cf. Aleodon</i>	x			
	<i>Exaeretodon</i>			x	
	<i>Ecteninion</i>			x	
	<i>Chiniquodon s.</i>			x	
	<i>Chiniquodon cf. t.</i>			x	
	<i>Probainognathus</i>			x	
	<i>Diegocanis</i>			x	
	<i>Eucynodontia nov</i>			x	
	<i>Chaliminia mustelooides</i>				x
	<i>Tessellatia bonapartei</i>				x
Rhynchosauria	Rhynchosaur indet.	x			
	<i>Scaphonyx</i>			x	
	<i>Teyumbaita</i>			x	
	<i>Hyperodapedon</i>			x	
Proterochampsidae	Proterochampsid indet.				
	<i>Chanaresuchus</i>	x		x	
	<i>Tropidosuchus</i>	x			
	<i>Gualosuchus</i>	x			
	<i>Proterochampsia</i>			x	
Testudinata	<i>Palaeochersis talampayensis</i>				x
Pseudosuchia	Pseudosuchia indet.	x	x	x	x
	<i>Tarjadia</i>	x			
	<i>Gracilisuchu</i>	x			

	<i>Luperosuchu</i>	x			
	<i>Aetosauroides</i>			x	
	<i>Sillosuchus</i>			x	
	<i>Saurosuchus</i>			x	
	<i>Trialestes</i>			x	
	<i>Venaticosuchus</i>			x	
	Crocodylomorpha indet.				x
	<i>Hemiprotosuchus leali</i>				x
	<i>Pseudohesperosuchus jachaleri</i>				x
	<i>Neoaetosauroides engaeus</i>				x
	<i>Riojasuchus tenuisceps</i>				x
	<i>Fasolasuchus tenax</i>				x
	<i>Coloradisuchus abelini</i>				x
	<i>Poposauridae</i>				x
Early Dinosauromorpha	Dinosauromorph indet.		x		
	<i>Lagerpeton</i>	x			
	<i>Lewisuchus</i>	x			
	<i>Lagosuchus</i>	x			
	Lagerpetidae			x	
	<i>Ignotosaurus</i>			x	
Dinosauria	Dinosauria indet.		x?		
	<i>Eoraptor</i>			x	
	<i>Herrerasaurus</i>			x	
	<i>Chromogisaurus</i>			x	
	<i>Sanjuansaurus</i>			x	
	<i>Eodromaeus</i>			x	
	<i>Pisanosaurus</i>			x	
	Theropoda indet.				x
	Sauropodomorpha indet.				x
	<i>Coloradisaurus brevis</i>				x
	<i>Lessemsaurus sauropoides</i>				x
	<i>Riojasaurus incertus</i>				x
	<i>Zupaysaurus rougieri</i>				x
	<i>Powellvenator podocitus</i>				x
	<i>Lessemsaurus sauropoides</i>				x

Diversification of non-mammaliaform cynodonts and the decline of synapsids and non-mammaliamorph cynodonts

Non-mammaliaform cynodonts reached a peak in abundance and diversity during the Triassic, with several radiation events of the two clades of derived cynodonts (Eucynodontia), Cynognathia, and Probainognathia, during the Middle and Late Triassic. Eucynodonts are conspicuous members of Carnian faunal associations, mainly in Gondwana, with a similar number of reported cynognathians and probainognathians. In contrast, Carnian cynodonts are only represented in Laurasia by three taxa: the traversodontid *Boreogomphodon*, the dromatheriid *Rewaconodon*, and the enigmatic *Adelobasileus*, which has been alternatively interpreted to be a derived non-mammaliaform probainognathian (dromatheriid) or an early-branching mammaliaform. By Norian times, a global change in cynodont diversity is recognized, with a notable decrease in the representation of cynognathians, due to the decline of the herbivorous traversodontids. Nevertheless, cynodonts continue to be better represented in Gondwanan strata, and Laurasian cynodonts remain scarce, only represented by the traversodontid *Arctotaversodon*, the dromatheriids *Dromatherium* and *Microconodon*, and the haramiyid *Thomasia*. On the other hand, during the late Norian and Rhaetian, probainognathians experienced a new radiation event represented by the highly specialized herbivorous tritylodontids, the small faunivorous derived prozostrodontians, and the first mammaliaforms. This diversification occurred in Laurasia, but only a few Gondwanan cynodonts have been reported. Except for a single report of an undetermined traversodontid from Brazil, highly specialized herbivorous cynodonts are absent in Norian and Rhaetian sediments from Gondwana as tritylodontids have not been found to date (see Abdala and Gaetano, 2018 and Abdala et al., 2020 for a review).

Dicynodontia was the other successful synapsid clade that proliferated during the Triassic, being that dicynodonts were very abundant and diverse until the Carnian. By the beginning of the Norian, they almost became extinct (e.g., Lucas, 1995; Fröbisch, 2009), with the only exception being a very fragmentary specimen from the Cretaceous of Australia (Thulborn and Turner, 2003 but see Knutsen and Oerlemans, 2020). In South America, only two species are recorded in early Norian levels, whereas nine are known from older Triassic units (Kammerer and Ordoñez, 2021).

Stratigraphic distribution of tetrapod through the sections and taphonomy

The early Carnian Chañares Formation has long been considered the richest fossil unit (Romer and Jensen, 1966; Rogers et al., 2001; Mancuso et al., 2014), with the highest abundance and diversity fossils come from the outcrops in Talampaya National Park. Two different patterns – attritional and mass mortality – were supported by taphonomic analysis (Rogers et al., 2001; Mancuso et al., 2014). The tetrapod record of the attritional accumulation is nearly 3:1:1 (cynodont:dicynodont:archosauriform), dominated by disarticulation and dispersion skeletons produced by scavengers and/or low-energy hydraulic flows (Mancuso et al., 2014). The mass mortality accumulation is nearly 20:1:7 (cynodont:dicynodont:archosauriform), and resulted in the preservation of a large quantity of completely or partially articulated skeletons and, on rare occasions, some sorting followed by rapid burial (Mancuso et al., 2014). Depositional environment and host-rock composition strongly influence preservation; thus, volcanism enhances preservation in two principal ways: by rapid burial and by creating a favorable diagenetic environment that promotes preservation. The better preservation observed in the Chañares tetrapod fossils included in the mass-mortality pathway is markedly linked with the rapid burial these remains have experienced (Mancuso et al., 2017). Moreover, the carbonatite ash chemically enhanced fossilization by providing an instant cement of sodium carbonate. The abundant supply of calcium carbonate favored alkaline soil chemistry in which bone apatite is relatively insoluble (Mancuso et al., 2017).

The middle Carnian Los Rastros Formation vertebrate fauna is represented by skeletal remains (fish and a temnospondyl amphibian) and trace fossils. Skeletal remains are not abundant; the lack of an autochthonous vertebrate fauna in the Los Rastros lake may result from unfavorable water chemistry during deposition. The occurrence of several episodes of Chlorococcales blooms in the Los Rastros succession may have depleted the phosphate concentration in the lake water and therefore resulted in the complete dissolution of vertebrate remains on the lake floor (Warren, 1986; Ottone et al., 2005; Ottone and Mancuso, 2006; Mancuso and Marsicano, 2008). The temnospondyl amphibian was the only tetrapod recorded as a body fossil and probably lived in the channel-floodplain environment of the fluvial system (Mancuso and Marsicano, 2008). In contrast, vertebrate trackways, which occur in the lake shoreline facies, are abundant and diverse, suggesting a diverse tetrapod fauna. The preservation of footprints on delta and palustrine facies has been enhanced by partial hardening of the trampled surface during subaerial exposure suggests fluctuating water levels (Marsicano et al., 2010).

The tetrapod fossil record of the late Carnian-early Norian Ischigualasto Formation is characterized by the highest abundance of material along the margins of the basin and rarer material toward the center of the basin. This spatial pattern was associated with sedimentary processes and geochemical conditions under the tectonic context that influences the accommodation space and sediment and water supply (Colombi et al., 2013). Most fossils are preserved in the floodplain facies with variable quality preservation, from isolated highly weathered specimens to complete well-preserved skeletons. The fossils found in channel facies are scarce and have variable preservational quality, including excellent preservation quality. Unit II recorded most of the tetrapod record in the Ischigualasto Formation, with a wide range of preservation quality and calcite as the main permineralized mineral. Unit III recorded less tetrapod than Unit II but more than Unit I and IV. The fossils in Unit III show evidence of long

exposure before burial and dominance of hematite precipitation on the surface and incite bones, as with fossils on Unit I (Colombi et al., 2013).

Finally, the lower levels of the Norian Los Colorados Formation preserve an abundant tetrapod record in the upper section. However, the lack of taphonomic studies makes it difficult to understand the relation of fossil records with sedimentological and climatic conditions.

Table S9. Summarized reference of paleontological record (vertebrate, macroflora, and microflora) in each unit of the Agua de la Peña Group, the Ischigualasto-Villa Unión Basin, Argentina

Formation	Vertebrate	Macroflora	Microflora
Los Colorados Fm.	Arcucci et al., 2004 Ezcurra and Apaldetti, 2011 Martinez et al., 2019 Leardi et al., 2020 Gaetano et al., 2022	Bonaparte, 1997	-
Ischigualasto Fm.	Martinez et al., 2011, 2013, 2015 Desojo et al., 2020 Colombi et al., 2021	Archangelsky and Brett, 1961, 1963 Archangelsky, 1968 Zamuner et al., 2001 Stipanicic and Marsicano, 2002 Colombi and Parrish, 2008 Drovandi et al., 2021	Cesari and Colombi, 2013; 2016
Los Rastros Fm.	Marsicano et al., 2004, 2007, 2010 Mancuso and Marsicano, 2008	Frenguelli, 1942, 1943, 1944, 1946, 1947, 1948 Groeber and Stipanicic, 1953 Zamuner et al., 2001 Stipanicic and Marsicano, 2002 Mancuso et al., 2009 Arce and Lutz, 2010, 2014 Lutz et al., 2011 Pedernera et al., 2020 Beltrán et al., 2021	Herbst, 1970, 1972 Zavattieri and Melchor, 1999 Ottone et al., 2005 Ottone and Mancuso, 2006
Chañares Fm.	Mancuso et al., 2014 Marsicano et al., 2016 Ezcurra et al., 2017 Mancuso and Irmis, 2020 Ordoñez et al., 2020	-	Perez Loinaze et al., 2018

Table S10. Taxonomic groups of macrofossils registered in the Agua de la Peña Group formations, the Ischigualasto-Villa Unión Basin, and ecological requirements and preferences are taken from Zhang et al. (2020); Ruffo Rey (2021).

Taxa	Moisture requirement	Temperatures preferences	Los Rastros Fm.	Ischigualasto Fm.	Los Colorados Fm.
Lycopsida (Pleuromeiales)	Hydrophytic	Megathermic	1	0	0
Equisetopsida	Hydrophytic	Mesothermic	7	1	0
Polypodiopsida (Osmundales)	Hydrophytic	Megathermic	3	1	1
Umkomasiales	Mesophytic	Megathermic	22	10	1
Peltaspermales	Hydrophytic	Mesothermic	3	2	0
Petriales	Hydrophytic	Mesothermic	1	0	0
Cycadales and Bennettitales	Hydrophytic	Megathermic	1	3	0
Ginkgoales	Hydrophytic	Mesothermic	6	1	0
Czekanowaskiales	Hydrophytic	Mesothermic	2	0	0
Voltziales (Heidiphyllum)	Hydrophytic	Mesothermic	7	1	0
Coniferales			1	2	1
Araucariaceae	Hydrophytic	Megathermic		1	1
Cupressaceae	Hydrophytic	Mesothermic		1	
Podocarpaceae	Hydrophytic	Mesothermic	1		
Gymnosperms uncertain affinity	-	-	15	0	0
Gnetales	Hydrophytic	Megathermic	3	3	0
Total			72	24	3

Table S11. Spore and pollen registered in each of the Agua de la Peña Group, the Ischigualasto-Villa Unión Basin, with their respective botanical affinities and ecological requirements and preferences from Zhang et al. (2020); Ruffo Rey (2021).

Taxa	Botanical affinity	Temprerature preference	Moisture requiremnt	Chañare s Fm.	Los Rastros Fm.	Ischigualasto Fm.
<i>'Rimaesporites' aquilonalis</i>	Voltziales	Megathermic	Mesophyte			X
<i>Abnormal pollen grains</i>	Indet.	-	-			X
<i>Accinctisporites</i>	Peltaspermales	Mesothermic	Hygrophyte		X	
<i>Alisporites</i>	Umkomasiales/ Peltaspermales	Megathermic	Mesophyte	X	X	X
<i>Anapiculatisporites</i>	Polypodiopsida	Megathermic	Mesophyte		X	X
<i>Annulispora</i>	Bryophytes	?	Hydrophylic			X
<i>Apiculatisporis</i>	Polypodiopsida	Megathermic	Mesophyte		X	
<i>Aratrisporites</i>	Pleuromeiales	Megathermic	Hygrophyte		X	X
<i>Araucariacites</i>	Araucariaceae	Megathermic	Mesophyte		X	X
<i>Ashmoriopollis</i>	Cycadales/Bennettitales	Megathermic	Mesophyte			X
<i>Baculatisporites</i>	Osmundaceae	Megathermic	Mesophyte		X	
<i>Birerisporites</i>	Polypodiopsida	Megathermic	Mesophyte		X	
<i>Botryococcus</i>	Freshwater alga	-	-		X	X
<i>Brachysaccus</i>	Coniferopsida?	-	-		X	X
<i>Cacheutasporites</i>	Uncertain cryptogam	-	-		X	
<i>Cadargasporites</i>	Polypodiopsida	Megathermic	Mesophyte	X	X	X
<i>Calamospora</i>	Equisetopsida	Mesothermic	Hygrophyte		X	X
<i>Carnisporites</i>	Polypodiopsida	Megathermic	Mesophyte			X
<i>Cedripites</i>	Coniferopsida indet.	-	-		X	
<i>cf. Callialasporites</i>	Uncertain gymnosperm	-	-			X
<i>cf. Carnisporites</i>	Polypodiopsida	Megathermic	Mesophyte			X
<i>cf. Craterisporites</i>	Lycopsids	Megathermic	Hygrophyte		X	
<i>cf. Cuneatisporites</i>	Uncertain gymnosperm	-	-		X	
<i>cf. Dacrycarpites .</i>	Uncertain gymnosperm	-	-		X	
<i>cf. Densipollenites</i>	Indet.	-	-		X	

<i>cf. Duplicisporites</i>	Coniferopsida indet.	-	-	X	X	
<i>cf. Kraeuselisporites</i>	Lycopsids	Megathermic	Hygrophyte	X	X	
<i>cf. Osmundacidores</i>	Polypodiopsida	Megathermic	Mesophyte		X	
<i>cf. Pustulatisporites</i>	Polypodiopsida	Megathermic	Mesophyte		X	
<i>cf. Vesicaspora</i>	Uncertain gymnosperm	-	-		X	
<i>Chordasporites</i>	Peltaspermales	Mesothermic	Hygrophyte		X	X
<i>Cingutriletes</i>	Bryophytes	?	Hydrophylic		X	X
<i>Cirratiradites</i>	Lycopsida - Selaginellales	Megathermic	Hygrophyte		X	
<i>Clavatisporites</i>	Lycopsids	Megathermic	Hygrophyte		X	X
<i>Con verrucosporites</i>	Polypodiopsida	Megathermic	Mesophyte	X		
<i>Crustaesporites</i>	Indet.	-	-	X		
<i>Cyathidites</i>	Polypodiopsida	Megathermic	Mesophyte	X		X
<i>Cycadopites</i>	Cycadales/ Bennettiales/ Ginkgoales	Megathermic	Mesophyte		X	X
<i>Cyclogranisporites</i>	Polypodiopsida	Megathermic	Mesophyte		X	
<i>Deltoispora</i>	Polypodiopsida	Megathermic	Mesophyte		X	
<i>Densoisporites</i>	Lycopsids	Megathermic	Hydrophylic		X	
<i>Dictyophyllidites</i>	Polypodiopsida	Megathermic	Mesophyte		X	X
<i>Ellipsovelatisporites</i>	Coniferopsida indet.	-	-	X		X
<i>Enzonalasporites</i>	Uncertain gymnosperm	-	-			X
<i>Equisetosporites</i>	Gnetales	Megathermic	Hygrophyte		X	X
<i>Falcisporites</i>	Umkomasiales/ Peltaspermales	Megathermic	Mesophyte	X	X	X
<i>Foveosporites</i>	Bryophytes	?	Hydrophylic			X
<i>Goubinispora</i>	Indet.	-	-		X	
<i>Granamonocolpites</i>	Indet.	-	-		X	
<i>Granulatisporites sp.</i>	Bryophytes?	?	Hydrophylic		X	
<i>Inapertisporites sp.</i>	Indet.	-	-		X	
<i>Inaperturopollenites</i>	Araucariaceae	Megathermic	Mesophyte		X	
<i>Indusiisporites</i>	Uncertain gymnosperm	-	-		X	
<i>Interulobites</i>	Bryophyta?	?	Hydrophylic	X		

<i>Klausipollenites</i>	Voltziales	Megathermic	Hygrophyte		X	
<i>Leiotrilletes</i>	Polypodiopsida	Megathermic	Mesophyte		X	
<i>Leptolepidites</i>	Lycopsida - Selaginellales	Megathermic	Hygrophyte	X	X	X
<i>Limatulasporites fossulatus/Limatulus complex</i>	Indet.	-	-	X		X
<i>Lophotrilletes</i>	Polypodiopsida	Megathermic	Mesophyte		X	X
<i>Lueckisporites</i>	Uncertain gymnosperm	-	-		X	X
<i>Lunatisporites</i>	Peltaspermales	Mesothermic	Hygrophyte		X	X
<i>Lundbladispora</i>	Lycopsids	Megathermic	Hydrophylic		X	X
<i>Lycospora</i>	Indet.	-	-		X	
<i>Megamonoporites</i>	Uncertain gymnosperm	-	-		X	
<i>Minutosaccus</i>	Podocarpaceae	Mesothermic	Mesophyte		X	X
<i>Monosulcites</i>	Cycadales/ Bennettitales/ Ginkgoales	Megathermic	Mesophyte		X	
<i>Neoraistrickia</i>	Lycopsids	Megathermic	Hygrophyte		X	
<i>Osmundacidites</i>	Polypodiopsida	Megathermic	Mesophyte		X	X
<i>Ovalipollis</i>	Voltziales	Megathermic	Hygrophyte	X		X
<i>Paraconcavisporites</i>	Indet.	-	-		X	
<i>Parcispores</i>	Uncertain gymnosperm	-	-		X	
<i>Partitisporites</i>	Coniferopsida indet.	-	-			X
<i>Patinasporites</i>	Voltziales	Megathermic	Mesophyte			X
<i>Perisporate spore indet</i>	Indet.	-	-	X		
<i>Pilasporites</i>	Freshwater alga	-	-		X	
<i>Plaesiodyction</i>	Freshwater alga	-	-		X	
<i>Platysaccus</i>	Umkomasiales	Megathermic	Mesophyte	X	X	X
<i>Playfordiaspora</i>	Pteridospermales	Mesothermic	Hygrophyte	X	X	X
<i>Podocarpidites</i>	Podocarpaceae	Mesothermic	Mesophyte	X	X	
<i>Polypodiidites</i>	Polypodiopsida?	Megathermic	Mesophyte			X
<i>Polypodiisporonites (ex Thymospora)</i>	Polypodiopsida	Megathermic	Mesophyte		X	

<i>Polysaccites</i>	Indet.	-	-		X	
<i>Protodiploxylinus</i>	Podocarpaceae	Mesothermic	Mesophyte	X	X	
<i>Protohaploxylinus</i>	Peltaspermales	Mesothermic	Hygrophyte	X	X	X
<i>Psilomonoporites</i>	Indet.	-	-		X	
<i>Pteruchipollenites</i>	Umkomasiales	Megathermic	Mesophyte		X	X
<i>Punctamonocolpites</i>	Indet.	-	-		X	
<i>Punctatisporites</i>	Polypodiopsida	Megathermic	Mesophyte		X	
<i>Quadraeculina</i>	Indet.	-	-			X
<i>Raistrikia</i>	Indet.	-	-		X	
<i>Regulatisporites</i>	Polypodiopsida	Megathermic	Mesophyte		X	
<i>Retitriletes</i>	Lycopodiaceae	Megathermic	Hygrophyte			X
<i>Retusotriletes</i>	Bryophytes	?	Hydrophylic		X	X
<i>Rimaesporites</i>	Voltziales	Megathermic	Mesophyte			X
<i>Rogalskaisporites</i>	Bryophytes	?	Hydrophylic			X
<i>Rugulatisporites</i>	Polypodiopsida	Megathermic	Mesophyte	X	X	X
<i>Samaropollenites</i>	Uncertain gymnosperm	-	-			X
<i>Scheuringipollenites</i>	Voltziales	Mesothermic	Hygrophyte	X		
<i>Schizosporis</i>	Freshwater alga	-	-		X	
<i>Scutaspores</i>	Indet.	-	-	X		
<i>Secarisporites</i>	Lycopsid - Selaginellales	Megathermic	Hygrophyte		X	
<i>Spheripollenites</i>	Coniferopsida indet.	-	-		X	
<i>Spore indet 1</i>	Indet.	-	-	X		
<i>Spore indet 2</i>	Indet.	-	-	X		
<i>Spore indet 3</i>	Indet.	-	-	X		
<i>Staurosaccites</i>	Voltziales	Megathermic	Hydrophylic			X
<i>Steevesipollenites</i>	Gnetales	Megathermic	Mesophyte		X	X
<i>Stereisporites</i>	Bryophytes	?	Hydrophylic		X	
<i>Striatella</i>	Polypodiopsida	Megathermic	Mesophyte			X
<i>Striatiti</i>	Indet.	-	-	X		
<i>Striatoabieites</i>	Peltaspermales	Mesothermic	Hygrophyte	X	X	X

<i>Striatopodocarpidites</i>	Uncertain gymnosperm	-	-	X	X	
<i>Sulcatisporites</i>	Voltziales	Mesothermic	Hygrophyte		X	
<i>Sulcosaccispora</i>	Umkomasiales	Megathermic	Mesophyte		X	
<i>Taurocusporites</i>	Bryophyta	?	Hydrophylic			X
<i>Tenuisaccites</i>	Indet.	-	-		X	
<i>Triadispora</i>	Voltziales	Megathermic	Xerophyte	X		X
<i>Trisaccites</i>	Indet.	-	-		X	
<i>Uvaesporites</i>	Lycopsids	Megathermic	Hygrophyte		X	X
<i>Vallaspores</i>	Voltziales	Megathermic	Mesophyte	X		X
<i>Variapollenites</i>	Coniferopsida indet.	-	-		X	
<i>Verrucosisporites</i>	Polypodiopsida	Megathermic	Mesophyte		X	
<i>Vesicaspora</i>	Uncertain gymnosperm	-	-		X	
<i>Vitreisporites</i>	Caytoniales	Megathermic	Mesophyte		X	
<i>Zonalasporites</i>	Indet.	-	-			X

Table S12. Description of the categories of moisture requirement and temperature preference. Taken from Zhang et al. (2020); Ruffo Rey (2021).

Moisture requirements	
Hydrophytes	aquatic plants that are completely or mostly submerged in water as well as being amphibious plants that grow both in water and in excessively wet habitats along the shorelines of water bodies
Hygrophytes	Plants living in excessively wet habitats with a high air and soil moisture, but usually no water stagnation on the surface, such as the lower tiers of wet forests, or open habitats with constantly wet soils and wet air
Mesophytes	Plants with the ability to resist periods of drought or regulate their water metabolism
Xerophytes	Plants that can resist long periods of drought and are living in well-drained soils.
Temperature tolerance	
Microthermic	Plants inhabiting cool regions with mean annual air temperatures below 14 °C.
Mesothermic	Plants inhabiting warm temperate regions (mean annual air temperature between 14 and 20 °C).
Megathermic	Plants inhabiting tropics and subtropics (mean annual air temperature above 20 °C).

Table S13. Tetrapod taxa database of Ischigualasto Formation. Taxa and specimens data based on Martínez et al. (2013) bins with complement of Desojo et al. (2020) data.

Table S14. Range of preferred temperatures and precipitation proposed in this contribution based on the inference of previous work (Dunne et al., 2020; Liu et al., 2021).

Preference Temperature	MAT °C
Low Temperature	>20
Middle Temperature	20< MAT >30
High Temperature	>30
Seasonal variation tolerance	
Low seasonal	<10
High seasonal	>20
Preference Precipitation	MAP mm/day
Low Precipitation	<1.5
Middle Precipitation	1.5> MAP <2
High Precipitation	>2
Seasonal variation tolerance	
Low seasonal	<0.1
High seasonal	>0.2

Table S15. Tetrapod groups registered in the Agua de la Peña Group formations, the Ischigualasto-Villa Unión Basin, and range of preferred temperatures and precipitation.

Taxonomic group	MAT (°C)	Season T(°C)	MAP (mm/day)	Season P (mm/day)	Chañares Fm.	Los Rastros Fm.	Ischigualasto Fm.	Los Colorados Fm.
Temnospondyli	High T	Low S	Middle P	Low S	0	1	2	0
Dicynodontia	Middle T	High S	Middle P	High S	3	1	2	1
Cynodontia	Middle T	High S	Middle P	High S	6	1	8	3
Rhynchosauria	High T	Low S	Middle P	Low S	1	0	3	0
Proterochampsidae	High T	Low S	Middle P	Low S	3	0	2	0
Testudinata	High T	Low S	Middle P	Low S	0	0	0	1
Pseudosuchia	High T	Low S	Middle P	Low S	4	1	6	8
Early Dinosauromorpha	Middle T	High S	High P	High S	3	1	2	0
Dinosauria	Middle T	High S	High P	High S	0	1	6	8

Correlation through basin

The Cerro Bola (CB) and Las Lajas (LL) sections are approximate ~12 km apart from one another (Figure 1). They record a thick pink volcaniclastic horizon at ~ 500 m in the CB section and ~ 800 m in the LL section (Desojo et al., 2020). This thick pink volcaniclastic horizon is used as a datum between sections. Moreover, a dated horizon (221.82 ± 0.10 Ma) near the top (~ 1000 m) of the LL section (Desojo et al., 2020) records a similar characteristic as a volcaniclastic horizon of the CB section (~ 700 m). Thus, both volcaniclastic horizons allow an admissible correlation between the two sections. In addition, the brief description of two dated volcaniclastic horizons (229.25 ± 0.10 Ma, 228.97 ± 0.22 Ma) in the lower part of the LL section (Desojo et al., 2020) allow a potential correlation of them with two volcaniclastic horizons around 120 and 180 m of the CB section.

On the other hand, Colombi et al. (2021) proposed the correlation of the LL section with the central area in Ischigualasto Provincial Park (IPP) (>80 km) based on dated horizons in both sections. Thus, the revised stratigraphic positions of the dated horizons in the LL section (229.25 ± 0.10 Ma, 228.97 ± 0.22 Ma) would be located 100 m higher than previously assumed (at ~200 m and ~300 m above the base of the formation), allowing correlation the second dated horizon with the horizon in IPP (228.91 ± 0.14 Ma) located 310 m above the base of the formation. Also, Colombi et al. (2021) disagreed with the thickness measured by the LL section and proposed a thickness not exceeding ~700 m, which was more similar to that of Colombi et al. (2017) previously published.

According to a new age model of the Ischigualasto-Villa Unión Basin (Irmis et al. in press), it is possible to correlate between the three areas (IPP, CB, and LL). The older recalculated age (231.4 ± 2.1 Ma) is located 10 m above the base of the Ischigualasto Formation at IPP. However, it must be located near the top (470 m) of the Los Rastros Formation at the CB (Figure S3). Upsection, three absolute ages (229.3 ± 0.10 Ma, 229.0 ± 0.2 Ma, 228.97 ± 0.37 Ma) are located around 190, 250, and 300 m respectively at IPP, whereas they are found around 120, 190, and 240 m respectively at CB and LL (Figure S3). We use the position at CB as the rule because the section in that area is continuing. Subsequently, the next recalculated age (225.9 ± 3.7 Ma) is located at 620 m at the IPP section and by correlation at 560 m at CB and LL (Figure S3). Below this level is the thick pink volcaniclastic used as a datum between CB and LL, also recorded at IPP around 580 m (Figure S3). Finally, the younger recalculated age (221.8 ± 0.10 Ma) is located around 650 at CB and LL (Figure 2). It must be located near the base (20 m) of the Los Colorados Formation at the IPP (Figure S3).

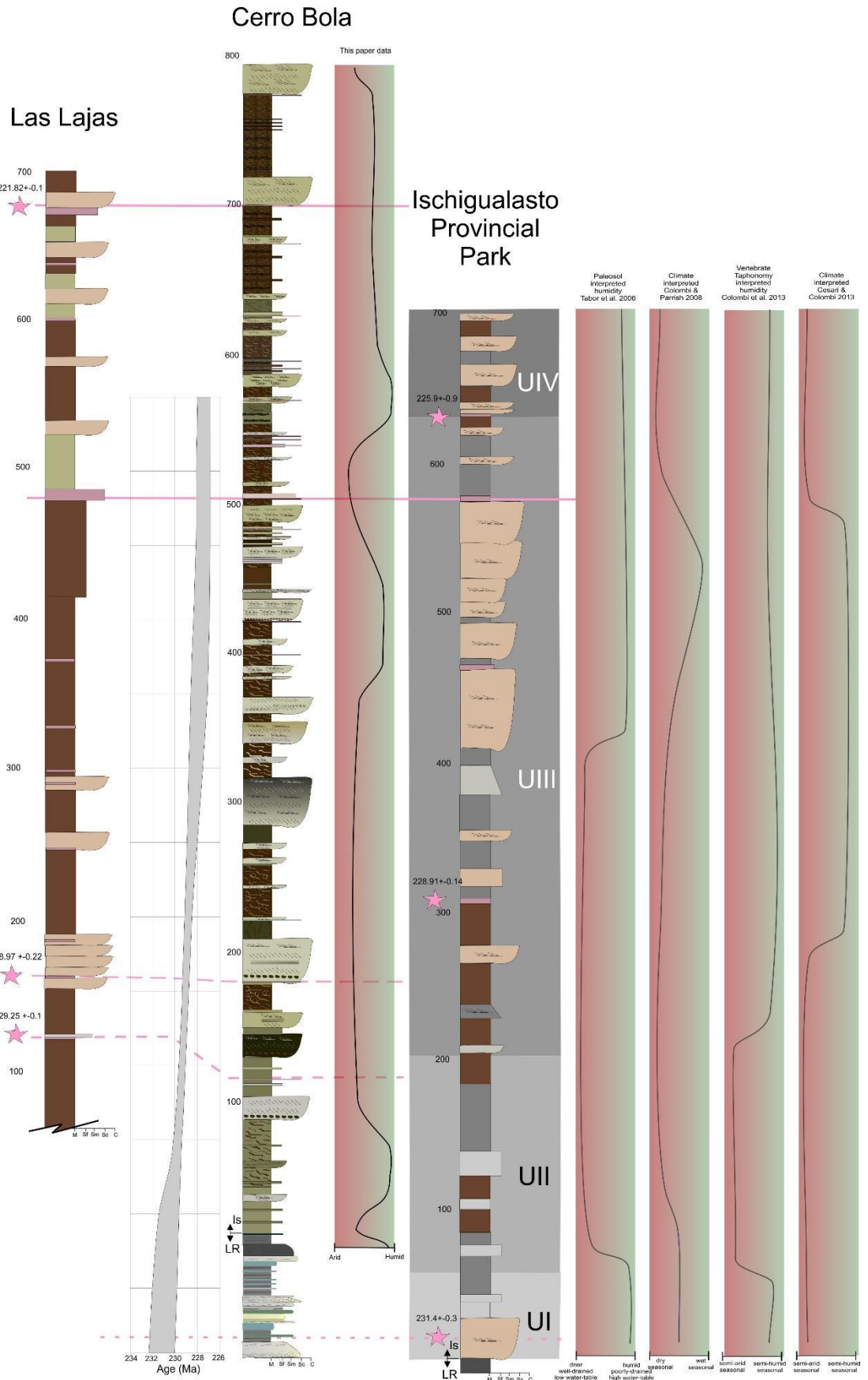


Figure S3. Correlation through basin of the Ischigualasto Formation. The Ischigualasto Provincial Park, Cerro Bola, and Las Lajas sections correlated based on the volcanioclastic horizon used as the datum between sections. Geochronologic age constraints for the Ischigualasto were modified from the preliminary age model with uncertainty envelope (grey shading) for the unit based on radioisotopic ages (Irmis et al., submitted). Absolute radioisotopic ages take from Desojo et al. 2020 and Colombi et al. 2021. Paleoclimate interpretations for the Ischigualasto Provincial Park take from Tabor et al., 2006; Colombi and Parish, 2008; Colombi et al., 2013; Cesari and Colombi, 2013.

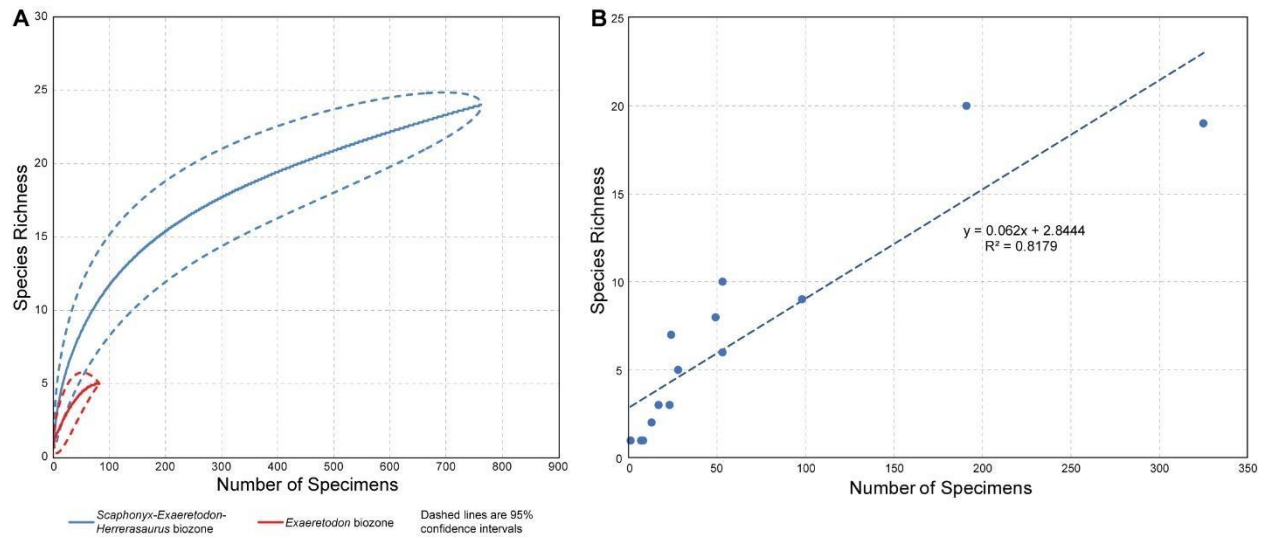


Figure S4. Comparison of Ischigualasto Formation tetrapod species richness to measures of specimen sampling. (A) Rarefaction analysis comparing the two main biozones. Note that at equivalent specimen numbers, the confidence intervals overlap broadly. (B) Plot of richness versus specimen number for each stratigraphic bin.

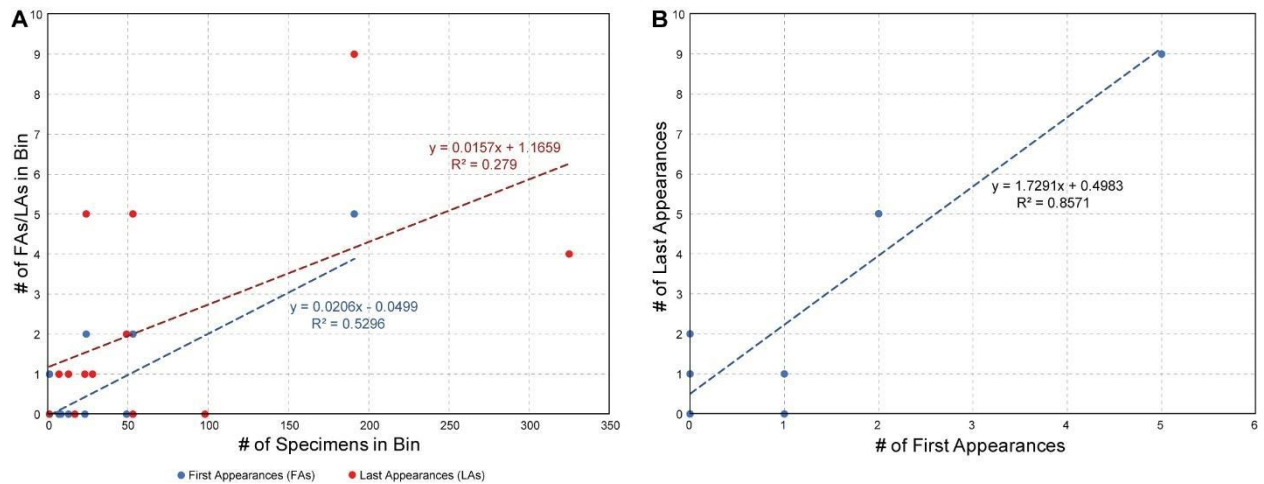


Figure S5. (A) Comparison of the number of first (FAs) and last appearances (LAs) in each stratigraphic bin of the Ischigualasto Formation to the number of specimens in those bins. (B) Comparison of FAs vs. LAs in each bin. As discussed in the main text, FAs from bin 1 and LAs from bin 14 are excluded from both plots because they are artifactual.

Table S16. Specimen data and calculated Adjusted Residuals (AR) comparing *Scaphonyx* to all other tetrapod taxa in the Ischigualasto Formation. AR values in bold are considered significant.

Stratigraphic Bin	# of Specimens		Adjusted Residuals	
	<i>Scaphonyx</i>	All other taxa	<i>Scaphonyx</i>	All other taxa
Zone 1	240	85	9.4148	-9.4148
Zone 2	118	73	2.6552	-2.6552
Zone 3	56	42	0.80337	-0.80337
Zone 4	22	31	-1.7815	1.7815
Zone 5	15	33	-3.1567	3.1567
Zone 6	5	43	-6.1347	6.1347
Zone 7	0	17	-4.4523	4.4523
Zone 8	0	23	-5.1973	5.1973
Zone 9	0	10	-3.4006	3.4006
Zone 10	0	16	-4.3168	4.3168
Zone 11	0	10	-3.4006	3.4006
Zone 12	0	7	-2.8401	2.8401
Zone 13	0	1	-1.0697	1.0697
Zone 14	0	8	-3.038	3.038

Chi squared test	
Chi2:	214.04
P:	1.77E-38

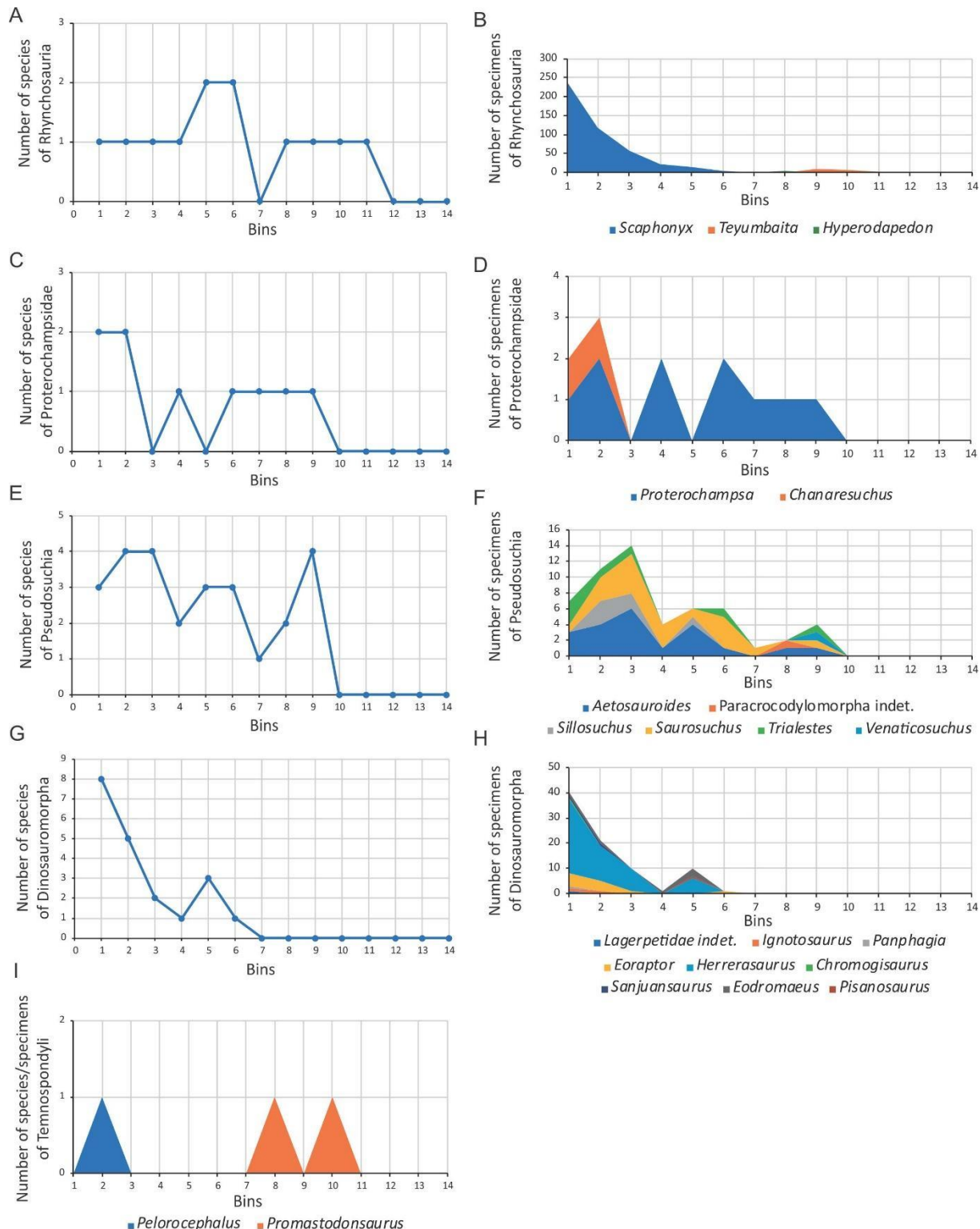


Figure S6. Temnospondyli and archosaurian diversity and abundance in the Ischigualasto Formation. Number of species and specimens of Rhynchosauria (A, B), Proterochampsidae (C, D), Pseudosuchia (E, F), Dinosauromorpha (G, H), and Temnospondyli (I) in the different time bins as defined by Martinez et al., 2013.

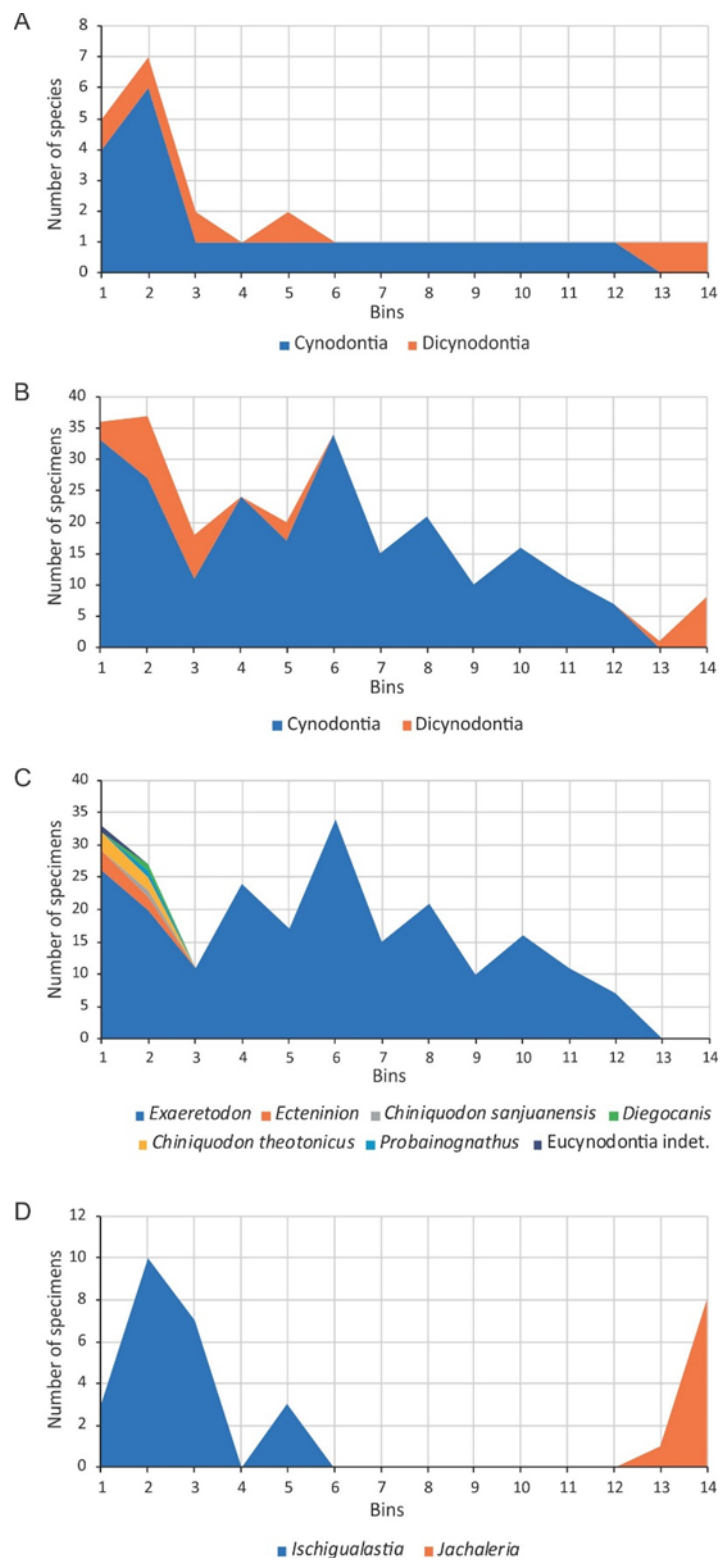


Figure S7. Synapsid diversity and abundance in the Ischigualasto Formation. Number of species (A) and specimens (B, C, D) in the different time bins as defined by Martinez et al., 2013.

References

- Abdala, Nestor Fernando; Gaetano, Leandro Carlos; The Late Triassic record of cynodonts: Time of innovations in the mammalian lineage; In: *The Late Triassic world: Earth in a time of transition*. Ed. L. Tanner. 407-445.
- Abdala, F., Gaetano, L.C., Martinelli, A.G., Soares, M.B., Hancox, P.J. and Rubidge, B.S. (2020). Non-mammaliaform cynodonts from western Gondwana and the significance of Argentinean forms in enhancing understanding of the group. *Journal of South American Earth Sciences* 104, 102884, 1-32.
- Arce, F.E. and Lutz, A.I. (2010). Fructificaciones de la Formación Los Rastros, Triásico Superior, Provincia de San Juan, Argentina. *Revista mexicana de Ciencias Geológicas*, 27(1), 31-42.
- Arce, F.E. and Lutz, A.I. (2014). *Acevedoa* nom. nov., a replacement name for *Andersonia* Arce and Lutz 2010 (*Insertae sedis*), preoccupied by *Andersonia* R. Br. 1810 (Plantae, Magnoliophyta, Ericaceae). *Revista mexicana de Ciencias Geológicas*, 31(1), 138-139.
- Archangelsky, S. (1968). Studies on Triassic fossil plants from Argentina. 4. The leaf genus *Dicroidium* and its possible relation to *Rhexoxylon* stems. *Palaeontology* 11, 500-512.
- Archangelsky, S. and Brett, D.W. (1961). Studies on Triassic fossil plants from Argentina. I. *Rhexoxylon* from the Ischigualasto Formation. *Philosophical Transactions of the Royal Society of London, Series B, Biological Sciences* 224(706), 1-19.
- Archangelsky, S. and Brett, D.W. (1963). Studies on Triassic fossil plants from Argentina. II. “*Michelilloa waltoni*” nov. gen. et sp. from the Ischigualasto Formation. *Annals of Botany* 27(105), 147-154.
- Arcucci, A.B., Marsicano, C.A. and Caselli, A.T. (2004). Tetrapod association and paleoenvironment of Los Colorados Formation (Argentina): a significant sample from western Gondwana at the end of the Triassic. *Geobios* 37, 555-568.
- Behrensmeyer, A.K. and Hook, R.W. (1992). *Paleoenvironmental contexts and taphonomic modes in the terrestrial fossil record*. In The evolutionary paleoecology of terrestrial plants and animals. (eds.) Behrensmeyer, A. K., Damuth, J. D., DiMichele, W.A., Potts, R., Sues, H. D. y Wing, S.L. (University of Chicago Press) 15-136.
- Beltrán, M., Bodnar, J. and Melchor, R. (2021). The genera *Heidiphyllum* and *Dordrechtites*, and associated fossil wood from the Triassic Ischichuca Formation, northwestern Argentina. *Journal of South American Earth Sciences*, 107, 103142.
- Bonaparte, J.F. (1972). Los tetrápodos del sector superior de la Formación Los Colorados, La Rioja, Argentina (Triásico superior). *Opera Lilloana* 22, 1-183.
- Bonaparte, J.F. (1997). El Triásico de San Juan-La Rioja Argentina y sus Dinosaurios: *Museo Argentino de Ciencias Naturales*, Buenos Aires.
- Césari, S.N. and Colombi, C.E. (2013). A new Late Triassic phytogeographical scenario in westernmost Gondwana. *Nature Communications* 4, 1-6.
- Césari, S.N. and Colombi, C.E. (2016). Palynology of the Late Triassic Ischigualasto Formation, Argentina: paleoecological and paleogeographic implications. *Palaeogeography, Palaeoclimatology, Palaeoecology* 449, 365-384.
- Colombi, C.E., Limarino, C.O., and Alcober, O.A. (2017). Allogenic controls on the fluvial architecture and fossil preservation of the Upper Triassic Ischigualasto Formation, NW Argentina. *Sedimentary Geology* 362, 1-16.
- Colombi, C.E., Martinez, R. N., Césari, S.N., Alcober, O.A., Limarino, C.O., and Montañez, I.P. (2021). A high-precision U-Pb zircon age constraints the timing of the faunistic and

- palynofloristic events of the Carnian Ischigualasto Formation, San Juan, Argentina. *Journal of South American Earth Sciences* 111, 103433.
- Colombi, C.E. and Parrish, J.T. (2008). Late Triassic environmental evolution in southwestern Pangea: plant taphonomy of the Ischigualasto Formation. *Palaios* 23, 778-795.
- Colombi, C.E., Rogers, R.R., and Alcober, O.A. (2013). Vertebrate taphonomy of the Ischigualasto Formation. Society of Vertebrate Paleontology Memoir 12, 31-50.
- Desojo, J. B., Fiorelli, L.E., Ezcurra, M.D., Martinelli, A.G., Ramezani, J., Da Rosa, Á. A., von Bacsko, M.B., Trotteyn, M.J., Montefeltro, F.C., Ezpeleta, M. and Langer, M. C. (2020). The Late Triassic Ischigualasto Formation at Cerro Las Lajas (La Rioja, Argentina): fossil tetrapods, high-resolution chronostratigraphy, and faunal correlations. *Scientific Reports* 10(1), 1-34.
- Dolby, J.H., and Balme, B.E. (1976). Triassic palynology of the Carnarvon Basin, western Australia. *Review of Palaeobotany and Palynology* 22, 105-168.
- Drovandi, J.M., Correa, G.A., Colombi, C.E. and Césari, S.N. (2021). *Dicroidium (Zuberia) zuberi* (Szajnocha) Archangelsky from exceptional Carnian leaf litters of the Ischigualasto Formation, westernmost Gondwana. *Historical Biology*, 1-14.
- Dunne, E.M., Farnsworth, A., Greene, S.E., Lunt, D.J., and Butler, R.J. (2021). Climatic drivers of latitudinal variation in Late Triassic tetrapod diversity. *Palaeontology* 64, 101-117.
- Ezcurra, M. D. and Apaldetti, C. (2012). A robust sauropodomorph specimen from the Upper Triassic of Argentina and insights on the diversity of the Los Colorados Formation. *Proceedings of the Geologists' Association* 123(1), 155-164.
- Ezcurra, M.D., Fiorelli, L.E., Martinelli, A.G., Rocher, S., von Bacsko, M.B., Ezpeleta, M., Taborda, J.R.A., Hechenleitner, E.M., Trotteyn, M.J. and Desojo, J.B. (2017). Deep faunistic turnovers preceded the rise of dinosaurs in southwestern Pangaea. *Nature Ecology & Evolution* 1, 1477-1483.
- Frenguelli, J. (1942). Contribuciones al conocimiento de la flora del Gondwana superior en la Argentina. *Chiropteris barrealensis* n. sp. *Notas del Museo La Plata* 7, *Paleontología* 51, 341-353.
- Frenguelli, J. (1943). Reseña crítica de los géneros atribuidos a la Serie de “*Thinnfeldia*”. *Revista del Museo de La Plata, nueva serie, Paleontología* 2, 225-342.
- Frenguelli, J. (1944). La serie del llamado Rético en el Oeste argentino. *Notas del Museo de La Plata* 9, *Geología* 30, 261-269.
- Frenguelli, J. (1947). El género “*Cladophlebis*” y sus representantes en la Argentina. *Anales del Museo de La Plata (nueva serie), Paleontología: sección B. Paleobotánica* 2, 5-74.
- Frenguelli, J. (1948). Estratigrafía y edad del llamado Rético en la Argentina. *Anales de la Sociedad Argentina de Estudios Geográficos, Sociedad Argentina de Estratigrafía Geológica* 8, 159-309.
- Fröbisch, J. (2009). Composition and similarity of global anomodont-bearing tetrapod faunas. *Earth-Sci. Rev.* 95, 119-157.
- Gaetano, L. C.; F. Abdala, F. D. Seoane, A. Tartaglione, M. Schulz, A. Otero, J. M. Leardi, C. Apaldetti, V. Krapovickas, and E. Steimbach. 2022. A new cynodont from the Upper Triassic Los Colorados Formation (Argentina, South America) reveals a novel paleobiogeographic context for mammalian ancestors. *Scientific Reports*, DOI: <https://doi.org/10.1038/s41598-022-10486-4>
- Gastaldo, R.A., Adendorff, R., Bamford, M., Labandeira, C.C., Neveling, J. and Sims, H. (2005). Taphonomic trends of macrofloral assemblages across the Permian-Triassic boundary, Karoo Basin, South Africa. *Palaios* 20(5), 479-497.

- Groeber, P. and Stipanicic, P. (1953). "Triásico", in Geografía de la República Argentina. Tomo II. Primera Parte, ed. P. Groeber (Sociedad Argentina de Estudio Geográficos, Buenos Aires), 13-141.
- Herbst, R. (1970). Estudio palinológico de la Cuenca Ischigualasto-Villa Unión, (Triásico), provincias de San Juan- La Rioja. I. Introducción. II. Monoaperturados. *Ameghiniana* 7, 83-97.
- Herbst, R. (1972). Estudio palinológico de la Cuenca Ischigualasto-Villa Unión (Triásico), provs. San Juan-La Rioja. III. Esporas triletes. *Ameghiniana* 9, 280-288.
- Herbst, R. (1965). Algunos esporomorfos del Triásico de Argentina. *Ameghiniana* 4:,141-155.
- Kammerer, C.F., and Ordoñez, M.A. (2021). Dicynodonts (Therapsida: Anomodontia) of South America. *Journal of South American Earth Sciences*, 108, 103171.
- Kent, D.V., Santi Malnis, P., Colombi. C.E., Alcober, O.A., and Martínez. R.N. (2014). Age constraints on the dispersal of dinosaurs in the Late Triassic from magnetostratigraphy of the Los Colorados Formation (Argentina). *Proceedings of the National Academy of Sciences* 111, 7958-7963.
- Knutsen, E. M. and Oerlemans, E. (2020) The last dicynodont? Re-assessing the taxonomic and temporal relationships of a contentious Australian fossil. *Gondwana Research* 77: 184-203 <https://doi.org/10.1016/j.gr.2019.07.011>.
- Leardi, J.M., Yanez, I., and Pol, D. (2020). South American Crocodylomorphs (Archosauria; Crocodylomorpha): A review of the early fossil record in the continent and its relevance on understanding the origins of the clade. *Journal of South American Earth Sciences* 104, 102780.
- Liu, J., Angielczyk, K.D., and Abdala, F. (2021). Permo-Triassic tetrapods and their climate implications. *Global and Planetary Change* 205, 103618, 1-9.
- Lucas, S.G. (1995). Triassic dicynodont biochronology. *Albertiana* 16, 33-40.
- Lutz, A., Gnaedinger, S., Mancuso, A. and Crisafulli, A. (2011). Paleoflora de la Formación los Rastros (Triásico medio), Provincia de San Juan, Argentina. Consideraciones taxonómicas y tafonómicas. *Ameghiniana* 48(4), 568-588.
- Mancuso, A.C., Previtera, E., Benavente, C.A., And Hernandez Del Pino S. (2017). Evidence of bacterial decay and early diagenesis in a partially-articulated tetrapod from the Triassic Chañares Formation. *Palaios* 32, 367-381
- Mancuso, A.C. (2009). Taphonomic analysis in lacustrine environments: two different contexts for Triassic lake paleofloras from Western Gondwana (Argentina). *Sedimentary Geology* 222(1-2), 149-159.
- Mancuso, A.C., Gaetano, L.C., Leardi J.M., Abdala, F., Arcucci, A.B., 2014. The Chañares Formation: a window to the palaeobiology of a Middle Triassic vertebrate fauna. *Lethaia* 47, 244–265.
- Mancuso, A.C., Irmis, R., 2020. A large-bodied Stahleckerine Dicynodont (Synapsida, Anomodontia) from the upper Triassic (Carnian) Chañares Formation (Argentina); new data for Triassic gondwanan biogeography. *Ameghiniana* 57, 45-57.
- Mancuso, A.C. and Marsicano, C.A. (2008). Paleoenvironments and taphonomy of a Triassic lacustrine system (Los Rastros Formation, central-western Argentina). *Palaios* 23, 535-547.
- Marsicano CA, Arcucci AB, Mancuso A and Caselli AT. (2004). Middle Triassic tetrapod footprints of southern South America. *Ameghiniana* 41,171-184.
- Marsicano, C. A., Mancuso, A. C., Palma, R. M. and Krapovickas, V. (2010). Tetrapod tracks in a marginal lacustrine setting (Middle Triassic, Argentina): taphonomy and significance. *Palaeoecology, Palaeogeography, Palaeoclimatology* 291, 388-399.

- Marsicano, C., Domnanovich, N. and Mancuso, A.C. (2007). Dinosaur origins: evidence from the footprint record. *Historical Biology* 19, 83-91.
- Marsicano, C., Irmis, R., Mancuso, A.C., Mundill, R. and Chemale, F. (2016). The precise temporal calibration of dinosaur origins. *Proceedings of the National Academy of Sciences of the United States of America* 113, 509-513.
- Martín-Closas, C., Gómez, B., 2004. Taphonomie des plantes et interprétations paléoécologiques. Une synthèse. *Geobios* 37(1), 65-88.
- Martínez, R. N., Alcober O. A., and Pol D. (2019). A new protosuchid crocodyliform (Pseudosuchia, Crocodylomorpha) from the Norian Los Colorados Formation, northwestern Argentina. *Journal of Vertebrate Paleontology*. DOI: 10.1080/02724634.2018.1491047.
- Martínez, R.N., Apaldetti, C., Alcober, O.A., Colombi, C.E., Sereno, P.C., Fernandez, E., Santi Malnis, P., Correa, G.A. and Abelin, D. (2013). Vertebrate succession in the Ischigualasto Formation. *Society of Vertebrate Paleontology Memoir* 12, 10-30.
- Martínez, R.N., Sereno, P. C., Alcober, O.A., Colombi, C.E., Renne, P.R., Montañez, I.P. and Currie, B.S. (2011). A basal dinosaur from the dawn of the dinosaur era in southwestern Pangaea. *Science* 331, 206210.
- Moore, D.M. and Reynolds, Jr., R.C. (1997). X-Ray Diffraction and the Identification and Analysis of Clay Minerals. Oxford University Press, Oxford, 337 pp.
- Nowak, H., Schneebeli-Hermann, E. and Kustatscher, E. (2019). No mass extinction for land plants at the Permian-Triassic transition. *Nature Communication* 10, 1-8.
- Ordoñez, A., Marsicano, C.A. and Mancuso, A.C. (2020). New material of Dinodontosaurus (Therapsida, Anomodontia) from west-central Argentina and a reassessment of the Triassic South American Dinodontosaurus Assemblage Zone. *Journal of South American Earth Sciences* 102597.
- Ottone, E.G. and Mancuso, A.C. (2006). Algas Chlorococcales como indicadores paleoambientales: nuevos datos de la Formación Los Rastros, Triásico Medio a Superior del centro-oeste de Argentina. *Revista del Museo Argentino de Ciencias Naturales, nueva serie* 8, 209-220.
- Ottone, E.G., Mancuso, A.C. and Resano, M. (2005). Miospores and chlorococcalean algae from the Los Rastros Formation, Middle to Upper Triassic of central-western Argentina. *Ameghiniana* 42, 347-362.
- Pedernera, T.E., Mancuso A.C., Ottone, E.G. and Benavente, C.A. (2020). Paleobotany of the Upper Triassic Los Rastros Formation, Ischigualasto-Villa Unión Basin, La Rioja, Argentina. *Journal of South American Earth Sciences* 102, 102660.
- Perez Loinaze, V.S., Vera, E.I., Fiorelli, L.E. and Desojo, J.B. (2018). Palaeobotany and palynology of coprolites from the Late Triassic Chañares Formation of Argentina: implications for vegetation provinces and the diet of dicynodonts. *Palaeogeography, Palaeoclimatology, Palaeoecology* 502, 31-51.
- Rogers, R., Swisher III, C., Sereno, P., Monetta, A., Forster, C., and Martínez, R. (1993). The Ischigualasto tetrapod assemblage (late Triassic, Argentina) and 40Ar/39Ar dating of dinosaur origins. *Science* 260, 794-797
- Rogers, R.R., Arcucci, A.B., Abdala, F., Sereno, P.C., Forster, C.A., and May, C.L. (2001). Paleoenvironment and taphonomy of the Chañares Formation tetrapod assemblage (Middle Triassic), northwestern Argentina: spectacular preservation in volcanogenic concretions. *Palaios* 16, 461-481.

- Romer, A.S. and Jensen, J.A. (1966). The Chañares (Argentina) triassic reptile fauna: sketch of the geology of the Rio Chanares-Rio Gualo region. *Breviora*, Museum of Comparative Zoology, Harvard, Cambridge, Mass.
- Rowe, H., Hughes, N. and Robinson, K. (2012). The quantification and application of handheld energy-dispersive x-ray fluorescence (ED-XRF) in mudrock chemostratigraphy and geochemistry. *Chemical Geology* 324-325, 122-131.
- Ruffo Rey, L.J.R. (2021). Vegetation dynamics of Cerro de Las Cabras Formation (Middle Triassic) from palynological assemblages and the Eco-Guild model: New paleoenvironmental and paleoclimatic interpretations. *Journal of South American Earth Sciences* 112, 103629.
- Spicer, R.A. (1991). *Plant Taphonomic Processes*. In *Taphonomy: Releasing the Data Locked in the Fossil Record* (eds.) Allison, P.A. and Briggs, D.E.G. (Topics in Geology, 9. Plenum Press, New York) 71-113.
- Stipanicic, P.N., (1969). El avance en los conocimientos del Jurásico argentino a partir del esquema de Groeber. *Revista de la Asociación Geológica Argentina* 224, 367-388.
- Stipanicic, P. N. (1983). The Triassic of Argentina and Chile. In *The Phanerozoic Geology of the world. The Mesozoic* (Eds) Moullade, M. and Nairn, A. E. M. Elsevier Scientific Publications, Amsterdam, 181-199.
- Stipanicic, P.N. and Marsicano (2002). *Léxico Estratigráfico de la Argentina. Volumen VIII. Triásico, Serie ``B''* (Asociación Geológica Argentina).
- Stipanicic, P.N. and Bonaparte, J. (1972). Cuenca Triásica de Ischigualasto-Villa Unión. In *Geología Regional Argentina*. (Ed.) Leanza, A.F. (Academia Nacional de Ciencias. Córdoba) 507-553.
- Stipanicic, P.N., Bonaparte, J., 1979. Cuenca Triásica de Ischigualasto-Villa Unión (provincias de La Rioja y San Juan). Segundo Simposio de Geología Regional Argentina, Academia Nacional de Ciencias. Córdoba 1, 523-575.
- Thulborn, T. and Turner, S. (2003). The last dicynodont: an Australian Cretaceous relict. *Proc. R. Soc. Lond. B* 270, 985-993.
- Warren, J.K. (1986). Shallow-water evaporitic environments and their source rock potential. *Journal of Sedimentary Petrology* 56, 442-454.
- Yrigoyen, M.R. and Stover, L.E. (1970). La palinología como elemento de correlación del Triásico en la Cuenca Cuyana. 4º Jornadas Geológicas Argentinas, (Mendoza), Actas 2: 427-447.
- Zamuner, A.B., Zavattieri, A.M., Artabe, A.E. and Morel, E.M. (2001). "Paleobotánica", in *El Sistema Triásico en la Argentina*, eds. A.E. Artabe, E.M. Morel, A.B. Zamuner (Fundación Museo de La Plata "Francisco Pascasio Moreno, La Plata"), 143-184.
- Zavattieri, A.M. and Melchor, R.N. (1999). Estudio palinológico preliminar de la Formación Ischichuca (Triásico), en su localidad tipo (Quebrada de Ischichuca Chica), Provincia de La Rioja, Argentina. *Asociación Paleontológica Argentina Publicación Especial* 6, 33-38.
- Zhang, J., Lenz, O.K., Hornung, J., Wang, P., Ebert, M. and Hinderer, M. (2020). Palynology and the eco-plant model of peat-forming wetlands of the upper Triassic Haojiagou formation in the Junggar basin, Xinjiang, NW China. *Palaeogeography, Palaeoclimatology, Palaeoecology* 556, 109888.